ECT*

EUROPEAN CENTRE FOR THEORETICAL STUDIES IN NUCLEAR PHYSICS AND RELATED AREAS
TRENTO, ITALY
Institutional Member of the European Expert Committee NUPECC

Castello di Trento ("Trint"), watercolor 19.8 x 27.7, painted by A. Dürer on his way back from Venice (1495). British Museum, London

QCD challenges in pp, pA and AA collisions at high energies

Trento, February 27 - March 3, 2017

Gluon Saturation Effects in Ultra - Peripheral Heavy Ion Collisions

Victor P. Goncalves

High and Medium Energy Group - UFPel - Brazil

Trento
28 Feb
2017

Basic Concepts

Basic Concepts

Consider a charged nucleus at rest. The associated electromagnetic field can be represented by:

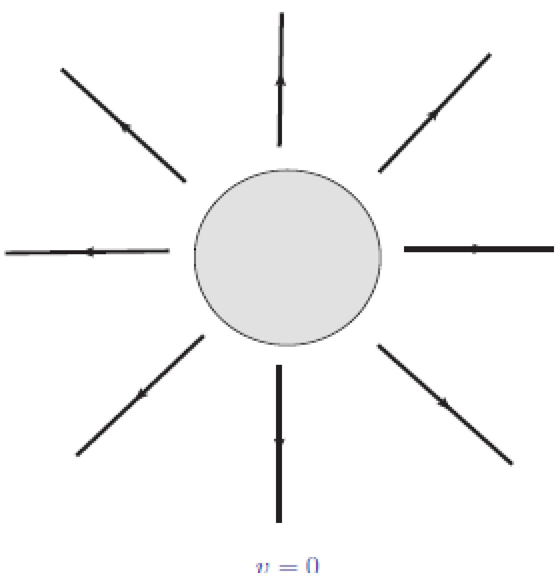

Basic Concepts

As the charged nucleus moves with nearly the speed of light, the electromagnetic field becomes transverse to its velocity.

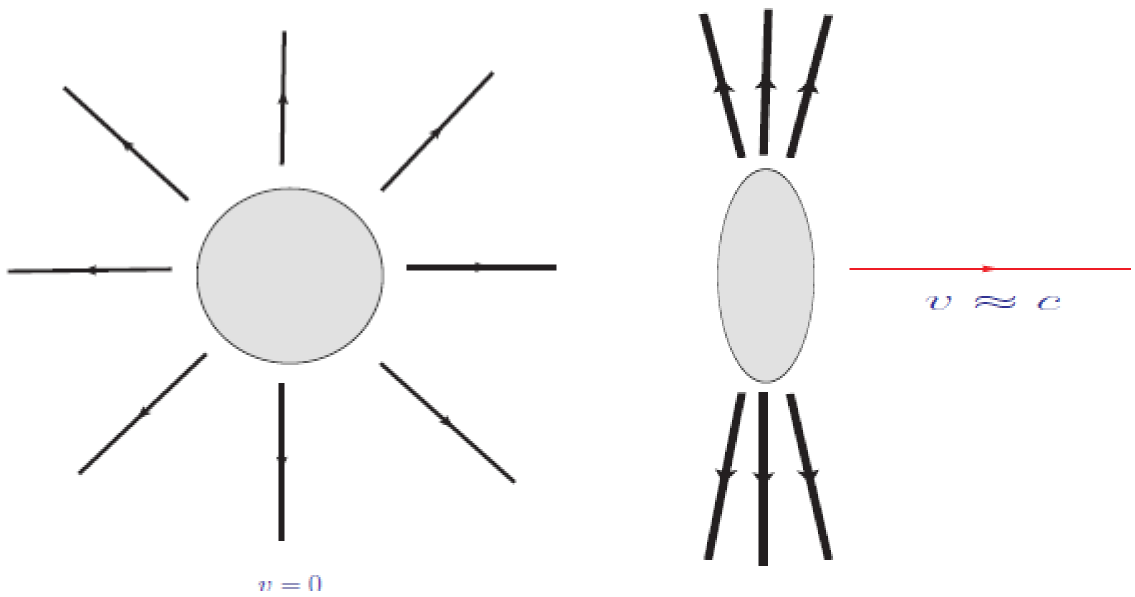

Basic Concepts

As the electric and magnetic fields associated to the nucleus take on the same absolute value, the electromagnetic field can be described by an equivalent flux of photons ([a]).

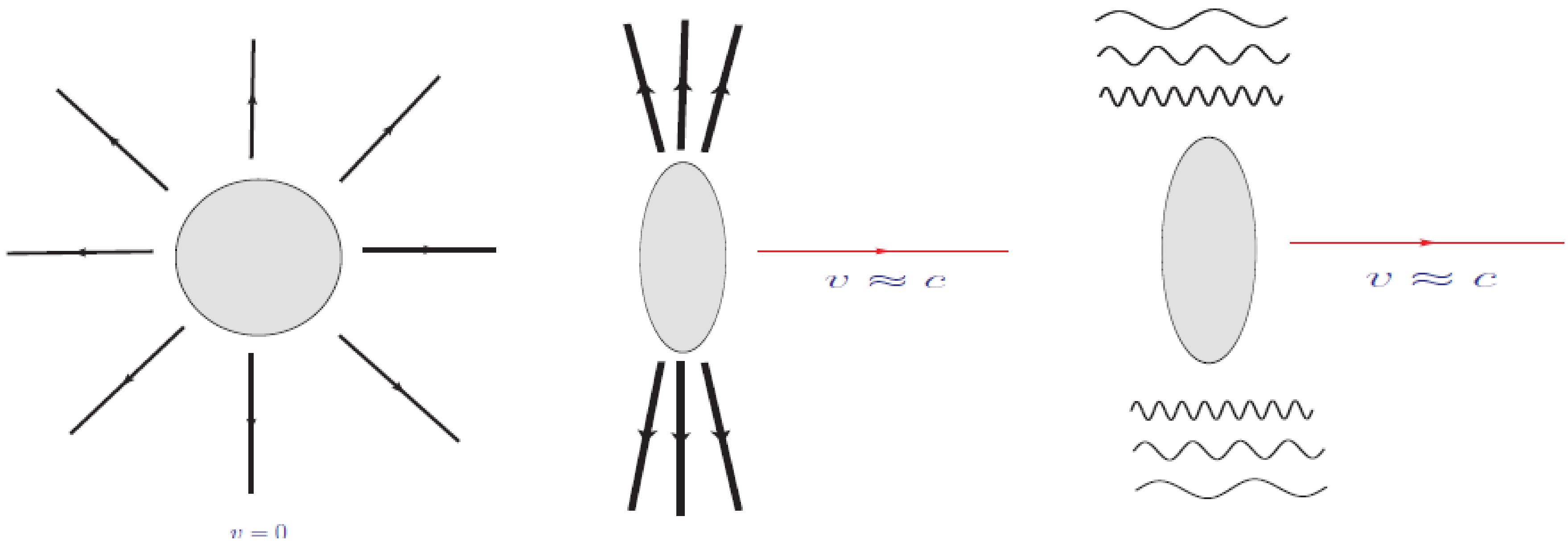

[a] E. Fermi (1924), E. J. Williams (1933), C. F. Von Weizacker (1934)

Basic Concepts

Thus the collision of two charged nuclei at large impact parameter (ultra - peripheral collisions) can be described as the collision of two equivalent swarms of photons.

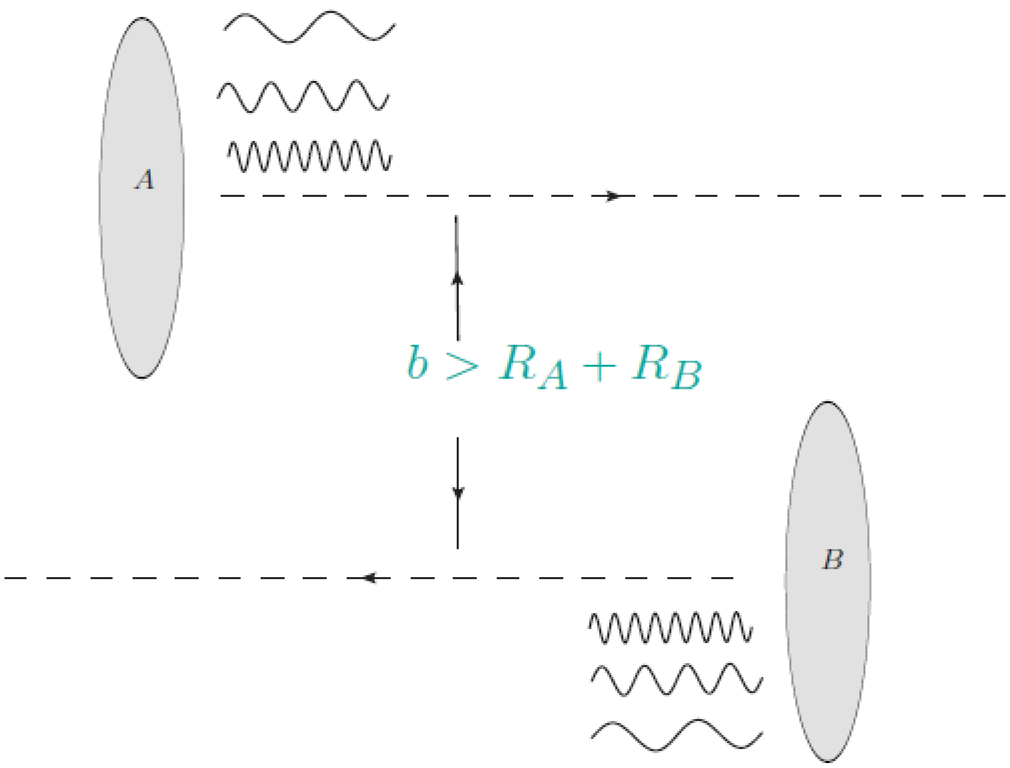

Basic Concepts

Thus the collision of two charged nuclei at large impact parameter (ultra - peripheral collisions) can be described as the collision of two equivalent swarms of photons.

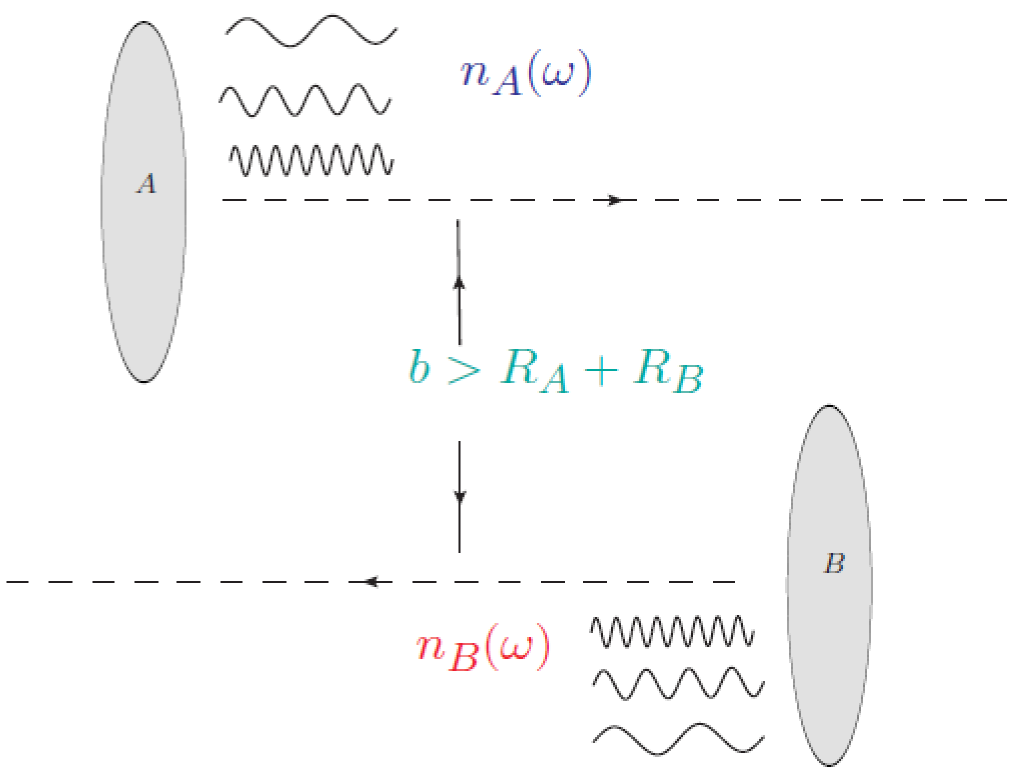

Basic Concepts

Thus the collision of two charged nuclei at large impact parameter (ultra - peripheral collisions) can be described as the collision of two equivalent swarms of photons.

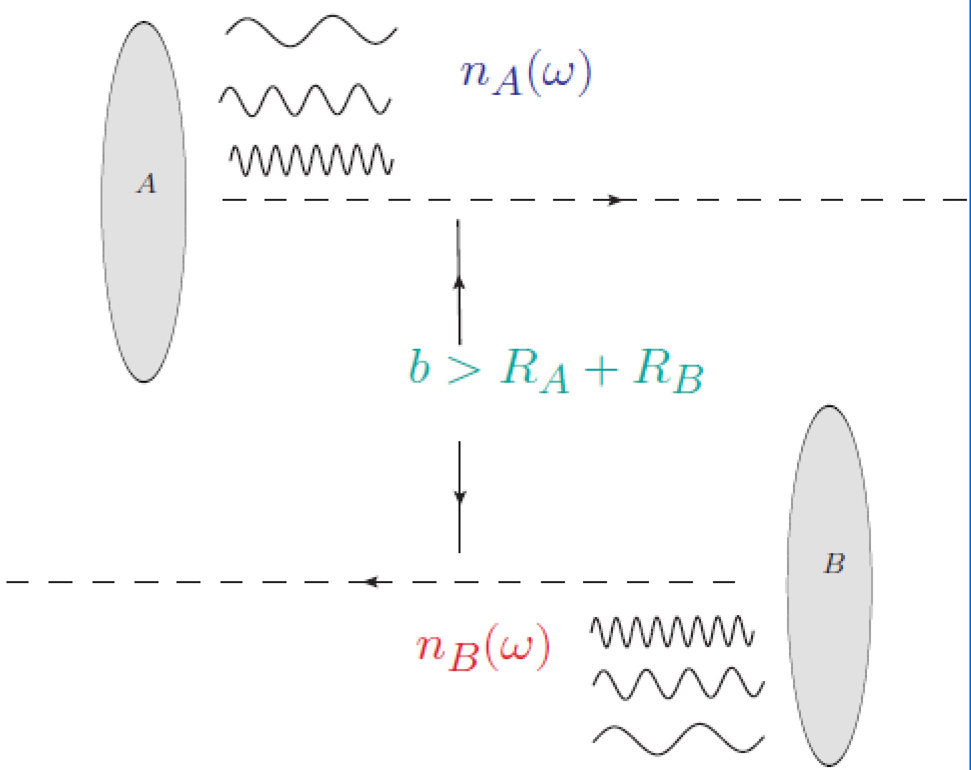

$$n(\omega) = \frac{(Ze)^2}{\pi\omega} \int_0^{+\infty} \frac{d^2k_\perp}{(2\pi)^2} \left[\frac{F\left(\left(\frac{\omega}{\gamma}\right)^2 + \vec{k}_\perp^{\,2} \right)}{\left(\frac{\omega}{\gamma}\right)^2 + \vec{k}_\perp^{\,2}} \right]^2 \cdot \vec{k}_\perp^{\,2}$$

Basic Concepts

Thus the collision of two charged nuclei at large impact parameter (ultra - peripheral collisions) can be described as the collision of two equivalent swarms of photons.

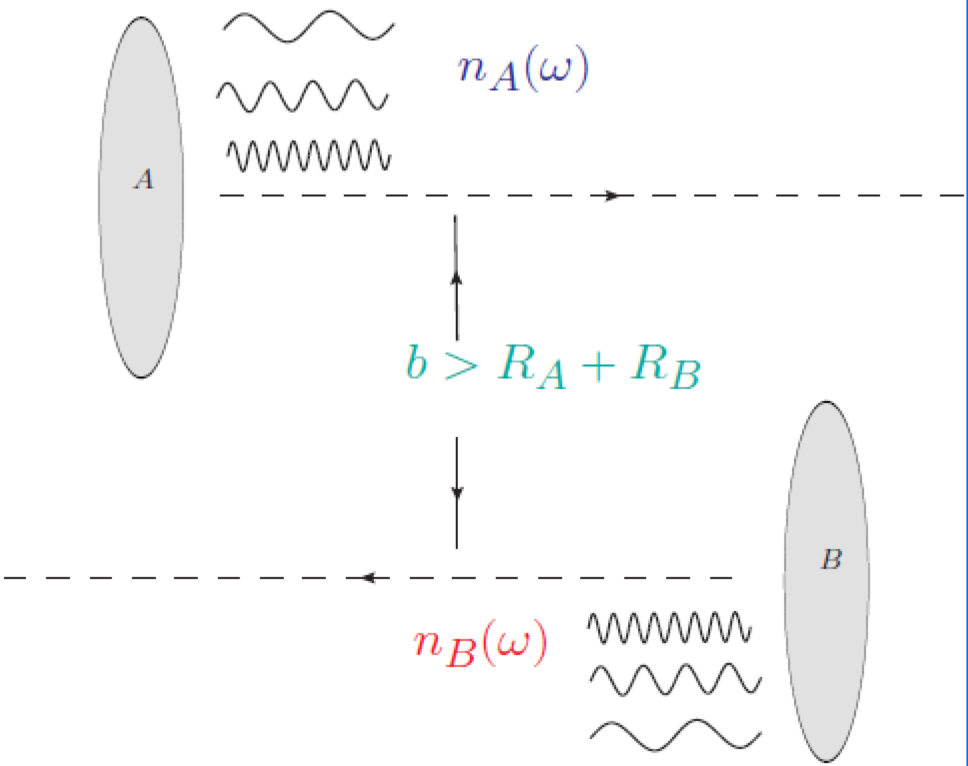

$$n(\omega) = \frac{(Ze)^2}{\pi\omega} \int_0^{+\infty} \frac{d^2k_\perp}{(2\pi)^2} \left[\frac{F\left(\left(\frac{\omega}{\gamma}\right)^2 + \vec{k}_\perp^{\,2} \right)}{\left(\frac{\omega}{\gamma}\right)^2 + \vec{k}_\perp^{\,2}} \right]^2 \cdot \vec{k}_\perp^{\,2}$$

Basic Concepts

Thus the collision of two charged nuclei at large impact parameter (ultra - peripheral collisions) can be described as the collision of two equivalent swarms of photons.

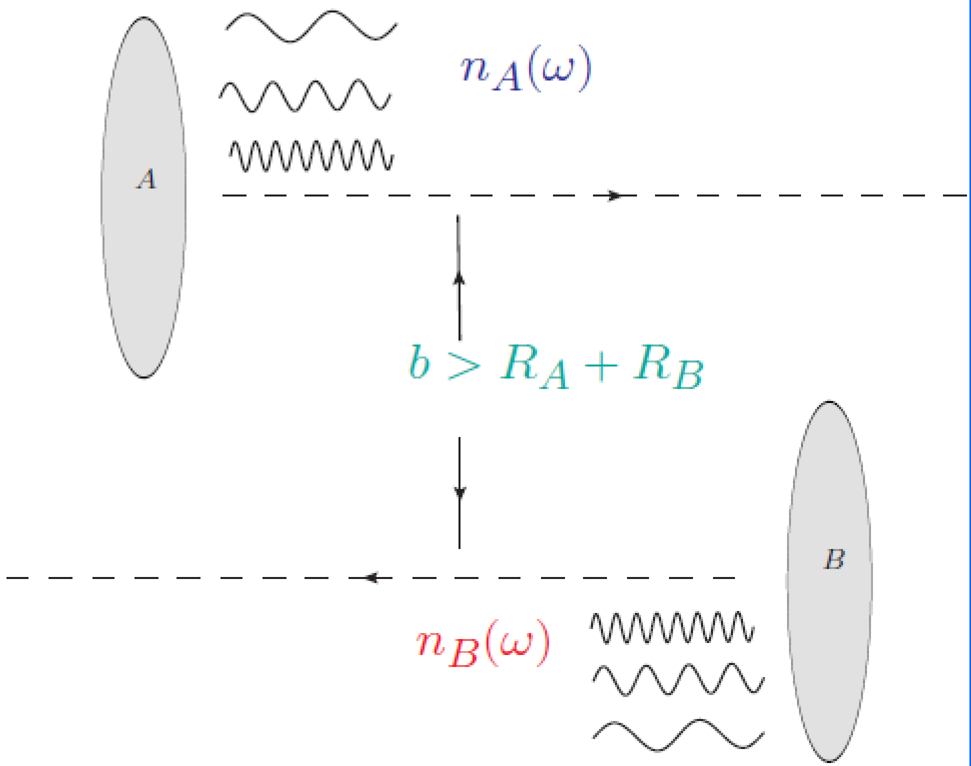

$$n(\omega) = \frac{(Ze)^2}{\pi\omega} \int_0^{+\infty} \frac{d^2k_\perp}{(2\pi)^2} \left[\frac{F\left(\left(\frac{\omega}{\gamma}\right)^2 + \vec{k}_\perp^{\,2} \right)}{\left(\frac{\omega}{\gamma}\right)^2 + \vec{k}_\perp^{\,2}} \right]^2 \cdot \vec{k}_\perp^{\,2}$$

Basic Concepts

Thus the collision of two charged nuclei at large impact parameter (ultra - peripheral collisions) can be described as the collision of two equivalent swarms of photons.

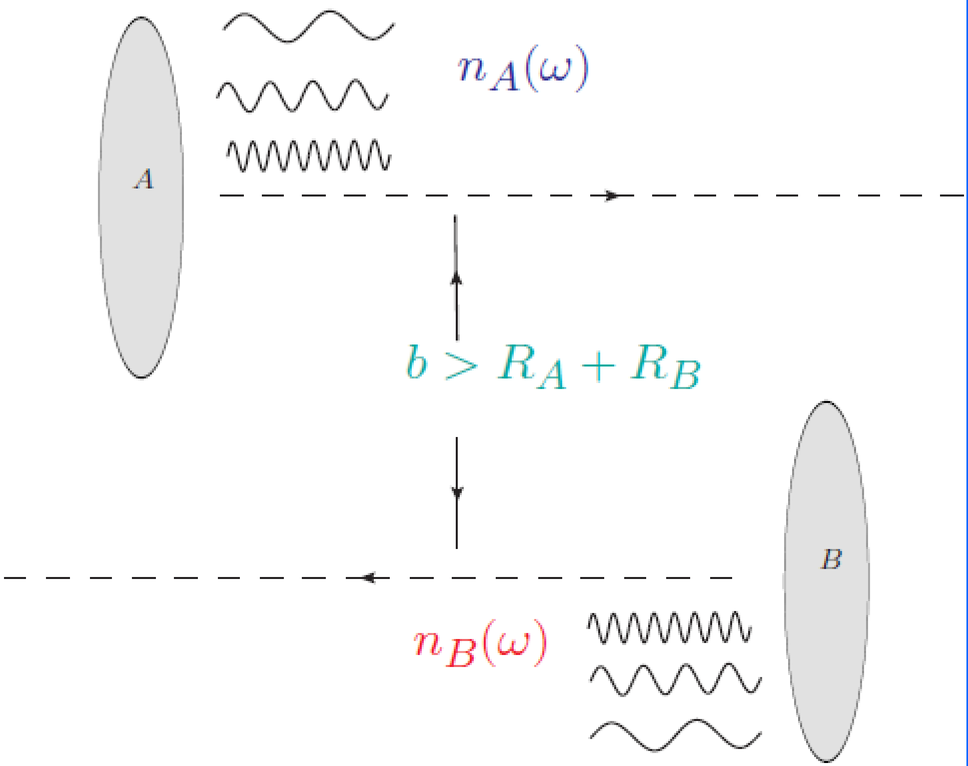

$$n(\omega) = \frac{(Ze)^2}{\pi\omega} \int_0^{+\infty} \frac{d^2k_\perp}{(2\pi)^2} \left[\frac{F\left(\left(\frac{\omega}{\gamma}\right)^2 + \vec{k}_\perp^{\,2} \right)}{\left(\frac{\omega}{\gamma}\right)^2 + \vec{k}_\perp^{\,2}} \right]^2 \cdot \vec{k}_\perp^{\,2}$$

Maximum photon energy:

$$\omega_{max} \approx \frac{\gamma}{R}$$

Basic Concepts

Thus the collision of two charged nuclei at large impact parameter (ultra - peripheral collisions) can be described as the collision of two equivalent swarms of photons.

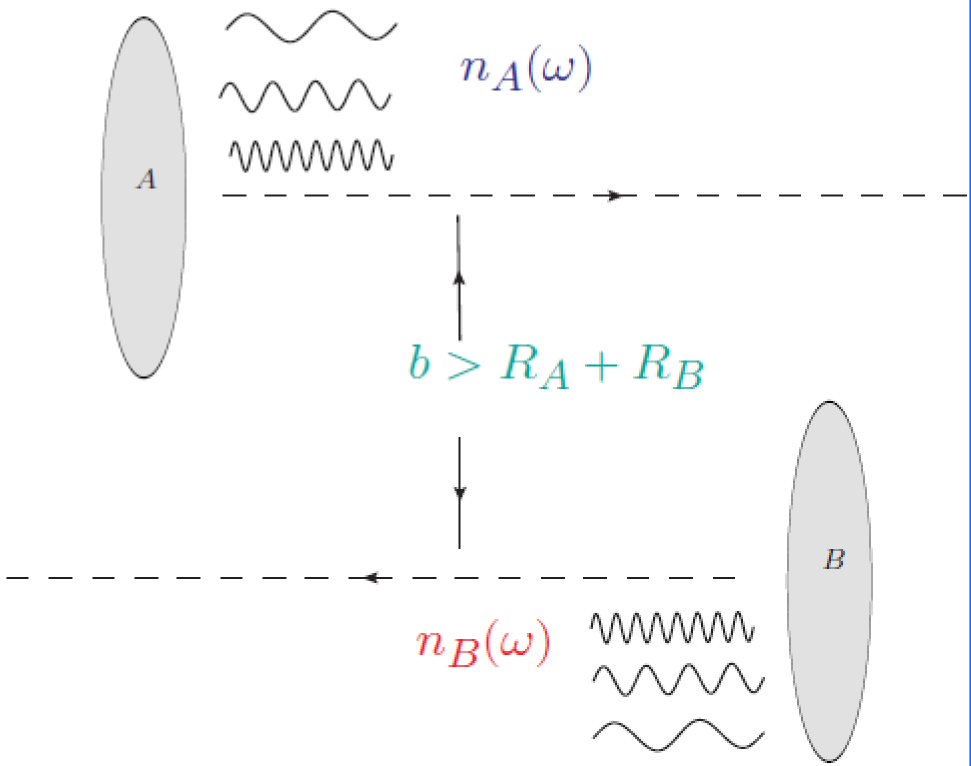

$$n(\omega) = \frac{(Ze)^2}{\pi\omega}\int_0^{+\infty}\frac{d^2k_\perp}{(2\pi)^2}\left[\frac{F\left(\left(\frac{\omega}{\gamma}\right)^2+\vec{k}_\perp^{\,2}\right)}{\left(\frac{\omega}{\gamma}\right)^2+\vec{k}_\perp^{\,2}}\right]^2\cdot\vec{k}_\perp^{\,2}$$

Maximum photon energy:

$$\omega_{max} \approx \frac{\gamma}{R}$$

The photon spectrum is harder for smaller charges!

Basic Concepts

Maximum center-of-mass energies:

$\gamma\gamma$ interactions: $s_{\gamma\gamma} = 4\,\omega_1\,\omega_2.$

γh interactions: $s_{\gamma h} = 2\,\omega\,\sqrt{s_{NN}}$

Considering that $\omega_{max} = \gamma / b_{min}$ we obtain that

$$\sqrt{s_{\gamma\gamma}^{max}} = 2\,\gamma / b_{min} \quad \text{and} \quad \sqrt{s_{\gamma h}^{max}} = \sqrt{\frac{2\,\gamma\sqrt{s_{NN}}}{b_{min}}}$$

System	$\sqrt{s_{NN}}$ (TeV)	$\mathcal{L}_{AB}$ ($\mathrm{cm}^{-2}\,\mathrm{s}^{-1}$)	$E_{\mathrm{beam1}} + E_{\mathrm{beam2}}$ (TeV)	γ	R_A (fm)	ω_{max} (GeV)	$\sqrt{s_{\gamma_N}^{\mathrm{max}}}$ (GeV)	$\sqrt{s_{\gamma\gamma}^{\mathrm{max}}}$ (GeV)	σ_{inel} (mb)
pp	14	10^{34}	7 + 7	7455	0.7	2450	8400	4500	110
pO	9.9	$2.7 \cdot 10^{30}$	7 + 3.5	5270	3.0	340	2600	690	480
pAr	9.4	$1.5 \cdot 10^{30}$	7 + 3.15	5000	4.1	240	2130	480	830
pPb	8.8	$1.5 \cdot 10^{29}$	7 + 2.76	4690	7.1	130	1500	260	2160
OO	7.0	$2 \cdot 10^{29}$	3.5 + 3.5	3730	3.0	240	1850	490	1500
ArAr	6.3	$0.6 \cdot 10^{29}$	3.15 + 3.15	3360	4.1	160	1430	320	2800
PbPb	5.5	$5 \cdot 10^{26}$	2.76 + 2.76	2930	7.1	80	950	160	7700

Basic Concepts

Maximum center-of-mass energies:

$\gamma\gamma$ interactions: $s_{\gamma\gamma} = 4\,\omega_1\,\omega_2.$

γh interactions: $s_{\gamma h} = 2\,\omega\,\sqrt{s_{NN}}$

Considering that $\omega_{max} = \gamma/b_{min}$ we obtain that

$$\sqrt{s_{\gamma\gamma}^{max}} = 2\,\gamma/b_{min} \quad \text{and} \quad \sqrt{s_{\gamma h}^{max}} = \sqrt{\frac{2\,\gamma\sqrt{s_{NN}}}{b_{min}}}$$

System	$\sqrt{s_{NN}}$ (TeV)	$\mathcal{L}_{AB}$ ($\text{cm}^{-2}\,\text{s}^{-1}$)	$E_{\text{beam1}} + E_{\text{beam2}}$ (TeV)	γ	R_A (fm)	ω_{max} (GeV)	$\sqrt{s_{\gamma N}^{\text{max}}}$ (GeV)	$\sqrt{s_{\gamma\gamma}^{\text{max}}}$ (GeV)	σ_{inel} (mb)
pp	14	10^{34}	7 + 7	7455	0.7	2450	8400	4500	110
pO	9.9	$2.7 \cdot 10^{30}$	7 + 3.5	5270	3.0	340	2600	690	480
pAr	9.4	$1.5 \cdot 10^{30}$	7 + 3.15	5000	4.1	240	2130	480	830
pPb	8.8	$1.5 \cdot 10^{29}$	7 + 2.76	4690	7.1	130	1500	260	2160
OO	7.0	$2 \cdot 10^{29}$	3.5 + 3.5	3730	3.0	240	1850	490	1500
ArAr	6.3	$0.6 \cdot 10^{29}$	3.15 + 3.15	3360	4.1	160	1430	320	2800
PbPb	5.5	$5 \cdot 10^{26}$	2.76 + 2.76	2930	7.1	80	950	160	7700

Basic Concepts

Maximum center-of-mass energies:

$\gamma\gamma$ interactions: $s_{\gamma\gamma} = 4\,\omega_1\,\omega_2.$

γh interactions: $s_{\gamma h} = 2\,\omega\,\sqrt{s_{NN}}$

Considering that $\omega_{max} = \gamma/b_{min}$ we obtain that

$$\sqrt{s_{\gamma\gamma}^{max}} = 2\,\gamma/b_{min} \quad \text{and} \quad \sqrt{s_{\gamma h}^{max}} = \sqrt{\frac{2\,\gamma\sqrt{s_{NN}}}{b_{min}}}$$

System	$\sqrt{s_{NN}}$ (TeV)	$\mathcal{L}_{AB}$ ($\mathrm{cm}^{-2}\,\mathrm{s}^{-1}$)	$E_{\mathrm{beam1}} + E_{\mathrm{beam2}}$ (TeV)	γ	R_A (fm)	ω_{max} (GeV)	$\sqrt{s_{\gamma_N}^{\mathrm{max}}}$ (GeV)	$\sqrt{s_{\gamma\gamma}^{\mathrm{max}}}$ (GeV)	σ_{inel} (mb)
pp	14	10^{34}	7 + 7	7455	0.7	2450	8400	4500	110
pO	9.9	$2.7 \cdot 10^{30}$	7 + 3.5	5270	3.0	340	2600	690	480
pAr	9.4	$1.5 \cdot 10^{30}$	7 + 3.15	5000	4.1	240	2130	480	830
pPb	8.8	$1.5 \cdot 10^{29}$	7 + 2.76	4690	7.1	130	1500	260	2160
OO	7.0	$2 \cdot 10^{29}$	3.5 + 3.5	3730	3.0	240	1850	490	1500
ArAr	6.3	$0.6 \cdot 10^{29}$	3.15 + 3.15	3360	4.1	160	1430	320	2800
PbPb	5.5	$5 \cdot 10^{26}$	2.76 + 2.76	2930	7.1	80	950	160	7700

Basic Concepts

Maximum center-of-mass energies:

$\gamma\gamma$ interactions: $s_{\gamma\gamma} = 4\,\omega_1\,\omega_2.$

γh interactions: $s_{\gamma h} = 2\,\omega\,\sqrt{s_{NN}}$

Considering that $\omega_{max} = \gamma/b_{min}$ we obtain that

$$\sqrt{s_{\gamma\gamma}^{max}} = 2\,\gamma/b_{min} \quad \text{and} \quad \sqrt{s_{\gamma h}^{max}} = \sqrt{\frac{2\,\gamma\sqrt{s_{NN}}}{b_{min}}}$$

System	$\sqrt{s_{NN}}$ (TeV)	$\mathcal{L}_{AB}$ ($\mathrm{cm^{-2}\,s^{-1}}$)	$E_{\mathrm{beam1}} + E_{\mathrm{beam2}}$ (TeV)	γ	R_A (fm)	$\omega_{\max}$ (GeV)	$\sqrt{s_{\gamma_N}^{\max}}$ (GeV)	$\sqrt{s_{\gamma\gamma}^{\max}}$ (GeV)	σ_{inel} (mb)
pp	14	10^{34}	7 + 7	7455	0.7	2450	8400	4500	110
pO	9.9	$2.7 \cdot 10^{30}$	7 + 3.5	5270	3.0	340	2600	690	480
pAr	9.4	$1.5 \cdot 10^{30}$	7 + 3.15	5000	4.1	240	2130	480	830
pPb	8.8	$1.5 \cdot 10^{29}$	7 + 2.76	4690	7.1	130	1500	260	2160
OO	7.0	$2 \cdot 10^{29}$	3.5 + 3.5	3730	3.0	240	1850	490	1500
ArAr	6.3	$0.6 \cdot 10^{29}$	3.15 + 3.15	3360	4.1	160	1430	320	2800
PbPb	5.5	$5 \cdot 10^{26}$	2.76 + 2.76	2930	7.1	80	950	160	7700

LHC = Photon collider

LHC = Photon collider

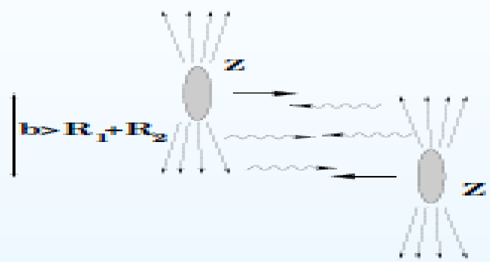

1. γh Processes: $\sigma(h_1 h_2 \to X) = n_h(\omega) \otimes \sigma^{\gamma h \to X}(W_{\gamma h})$
2. $\gamma\gamma$ Processes: $\sigma(h_1 h_2 \to X) = n_1(\omega) \otimes n_2(\omega) \otimes \sigma^{\gamma\gamma \to X}(W_{\gamma\gamma})$

Center of mass energies

LHC	pp	$W_{\gamma p} \lesssim 8390$ GeV	$W_{\gamma\gamma} \lesssim 4504$ GeV
LHC	$pPb(Ar)$	$W_{\gamma A} \lesssim 1500\,(2130)$ GeV	$W_{\gamma\gamma} \lesssim 260\,(480)$ GeV
LHC	$PbPb$	$W_{\gamma A} \lesssim 950$ GeV	$W_{\gamma\gamma} \lesssim 160$ GeV
HERA	ep	$W_{\gamma p} \lesssim 200$ GeV	–

Photoproduction in pp collisions at LHC probes photon – hadron center – of – mass energies one order of magnitude larger than HERA.

LHC = Photon collider

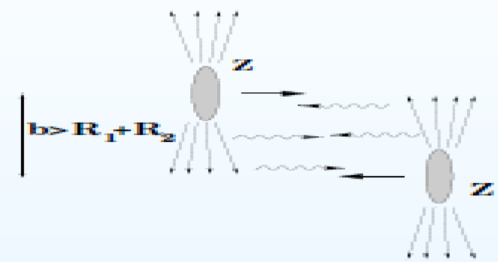

1. γh Processes: $\sigma(h_1 h_2 \to X) = n_h(\omega) \otimes \sigma^{\gamma h \to X}(W_{\gamma h})$
2. $\gamma\gamma$ Processes: $\sigma(h_1 h_2 \to X) = n_1(\omega) \otimes n_2(\omega) \otimes \sigma^{\gamma\gamma \to X}(W_{\gamma\gamma})$

Center of mass energies

LHC	pp	$W_{\gamma p} \lesssim 8390$ GeV	$W_{\gamma\gamma} \lesssim 4504$ GeV
LHC	$pPb(Ar)$	$W_{\gamma A} \lesssim 1500\,(2130)$ GeV	$W_{\gamma\gamma} \lesssim 260\,(480)$ GeV
LHC	$PbPb$	$W_{\gamma A} \lesssim 950$ GeV	$W_{\gamma\gamma} \lesssim 160$ GeV
HERA	ep	$W_{\gamma p} \lesssim 200$ GeV	–

Photoproduction in pA and AA collisions at LHC probes a unexplorated regime of photon – nucleus center of mass energies.

LHC = Photon collider

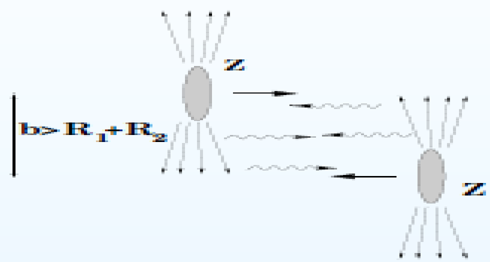

1. γh Processes: $\sigma(h_1 h_2 \to X) = n_h(\omega) \otimes \sigma^{\gamma h \to X}(W_{\gamma h})$
2. $\gamma\gamma$ Processes: $\sigma(h_1 h_2 \to X) = n_1(\omega) \otimes n_2(\omega) \otimes \sigma^{\gamma\gamma \to X}(W_{\gamma\gamma})$

Center of mass energies

LHC	pp	$W_{\gamma p} \lesssim 8390$ GeV	$W_{\gamma\gamma} \lesssim 4504$ GeV
LHC	$pPb(Ar)$	$W_{\gamma A} \lesssim 1500\,(2130)$ GeV	$W_{\gamma\gamma} \lesssim 260\,(480)$ GeV
LHC	$PbPb$	$W_{\gamma A} \lesssim 950$ GeV	$W_{\gamma\gamma} \lesssim 160$ GeV
HERA	ep	$W_{\gamma p} \lesssim 200$ GeV	–

Photon - induced interactions at LHC allows to study the high energy regime of QCD (Small - x Physics).

Hadronic structure at high energies

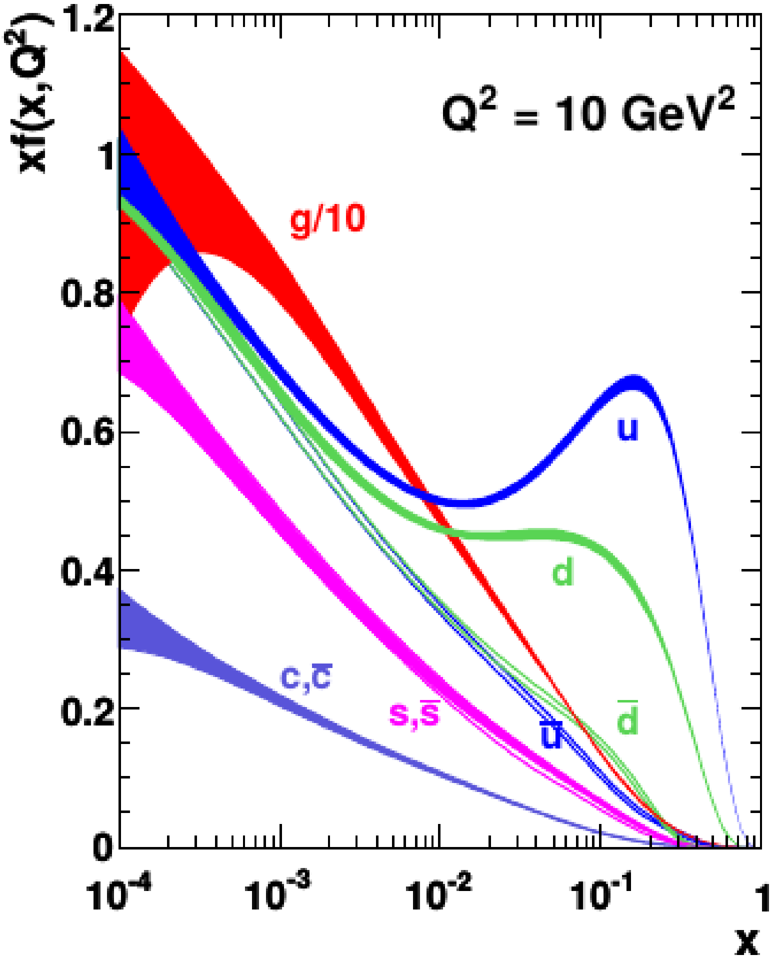

- Proton structure at high energies (small values of x) is dominated by gluons;
- Linear QCD Evolution equations (DGLAP/BFKL) predict a power growth of gluon distribution at small -x;
- Large uncertainty on the behaviour at small -x;
- The current data included in the global analysis does not constrain the gluon distribution at high energies.

Hadronic structure at high energies

$$R_g \equiv \frac{x g_A(x, Q^2)}{A \cdot x g_p(x, Q^2)}$$

- No nuclear effects $\Rightarrow R_g = 1$.

$R = f_{j/A}(x,Q^2)/[A f_{j/N}(x,Q^2)]$

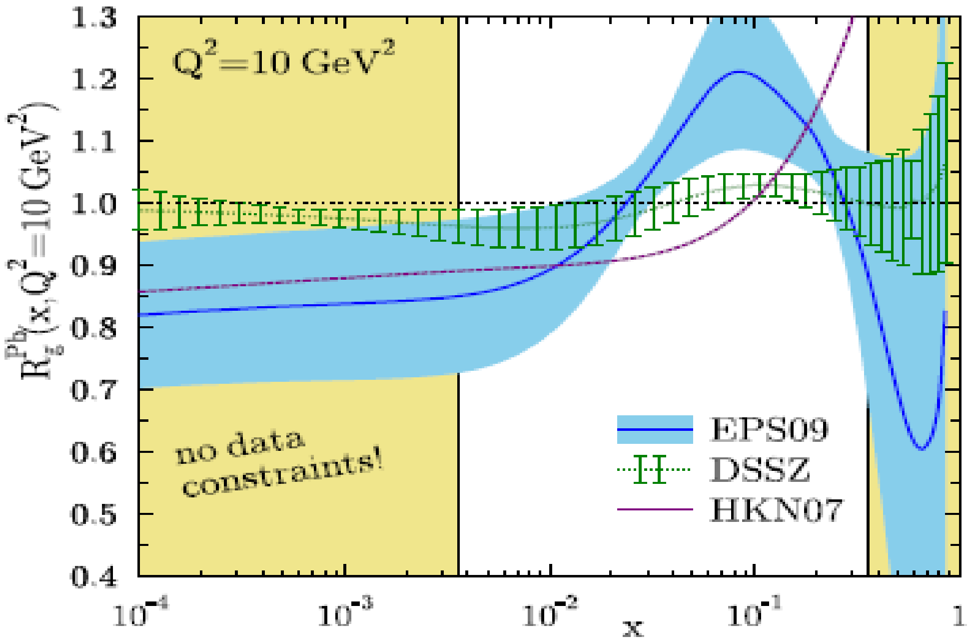

Eskola, Puukkunen, arXiv:1401.2345

- The current electron - ion experimental data does not constrain the small -x behaviour;
- Large theoretical uncertainty present in the kinematical range probed by LHC.

Diffractive vector meson photoproduction in UPHIC: Probing the gluon distribution

$$\frac{d\sigma\,[h_1 + h_2 \to h_1 \otimes V \otimes h_2]}{dY} = \left[\omega\frac{dN}{d\omega}|_{h_1}\,\sigma_{\gamma h_2 \to V\otimes h_2}\,(\omega)\right]_{\omega_L} + \left[\omega\frac{dN}{d\omega}|_{h_2}\,\sigma_{\gamma h_1 \to V\otimes h_1}\,(\omega)\right]_{\omega_R}$$

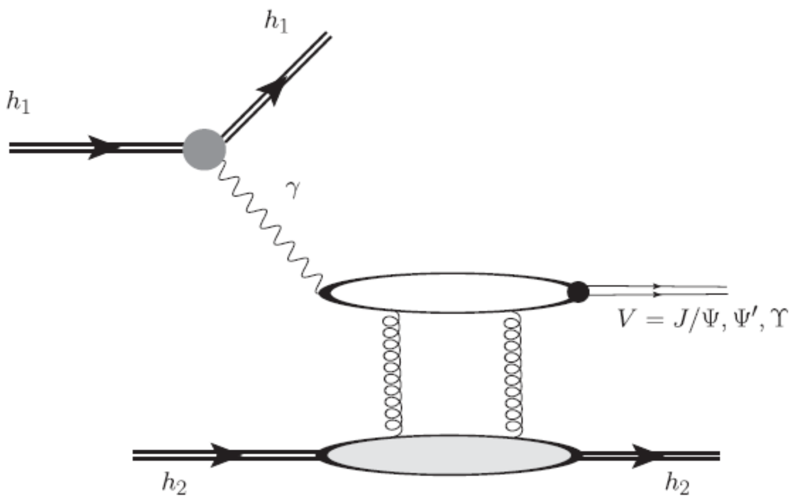

[a] VPG, Bertulani, PRC65, 054905 (2002)

Diffractive vector meson photoproduction in UPHIC: Probing the gluon distribution

$$\frac{d\sigma\left[h_1+h_2\to h_1\otimes V\otimes h_2\right]}{dY}=\left[\omega\frac{dN}{d\omega}\Big|_{h_1}\sigma_{\gamma h_2\to V\otimes h_2}(\omega)\right]_{\omega_L}+\left[\omega\frac{dN}{d\omega}\Big|_{h_2}\sigma_{\gamma h_1\to V\otimes h_1}(\omega)\right]_{\omega_R}$$

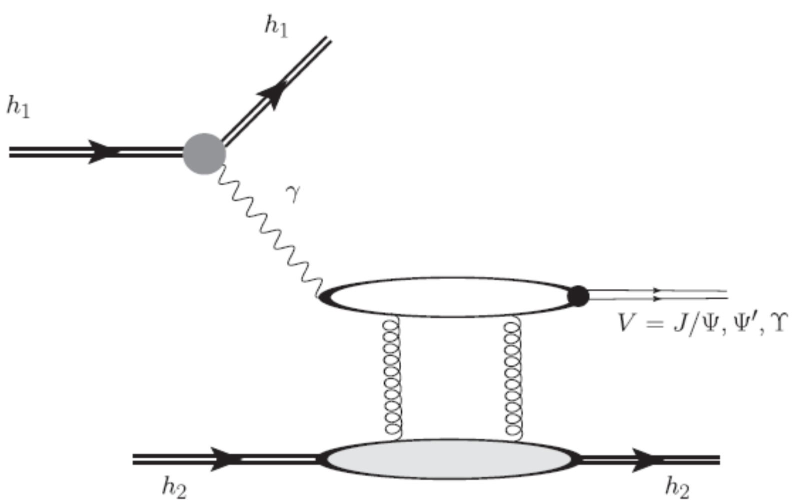

At leading order in LL(1/x) approx.:

$$\frac{d\sigma^{\gamma h\to Vh}}{dt}\Big|_{t=0}=\mathcal{N}\frac{\pi^3\Gamma_{e^+e^-}M_V^3}{48\alpha_{em}}\left[\frac{\alpha_s(\bar{Q}^2)}{\bar{Q}^4}xg_h(x,\bar{Q}^2)\right]^2$$

Cross section is proportional to the square of the hadron gluon distribution at $x=4\overline{Q}^2/W^2$

[a] VPG, Bertulani, PRC65, 054905 (2002)

Diffractive vector meson photoproduction in UPHIC: Probing the gluon distribution

$$\left.\frac{d\sigma^{\gamma h\to Vh}}{dt}\right|_{t=0} = \mathcal{N}\frac{\pi^3\Gamma_{e^+e^-}M_V^3}{48\alpha_{em}}\left[\frac{\alpha_s(\bar{Q}^2)}{\bar{Q}^4}xg_h(x,\bar{Q}^2)\right]^2$$

$$\bar{Q} = \xi M_V/2$$

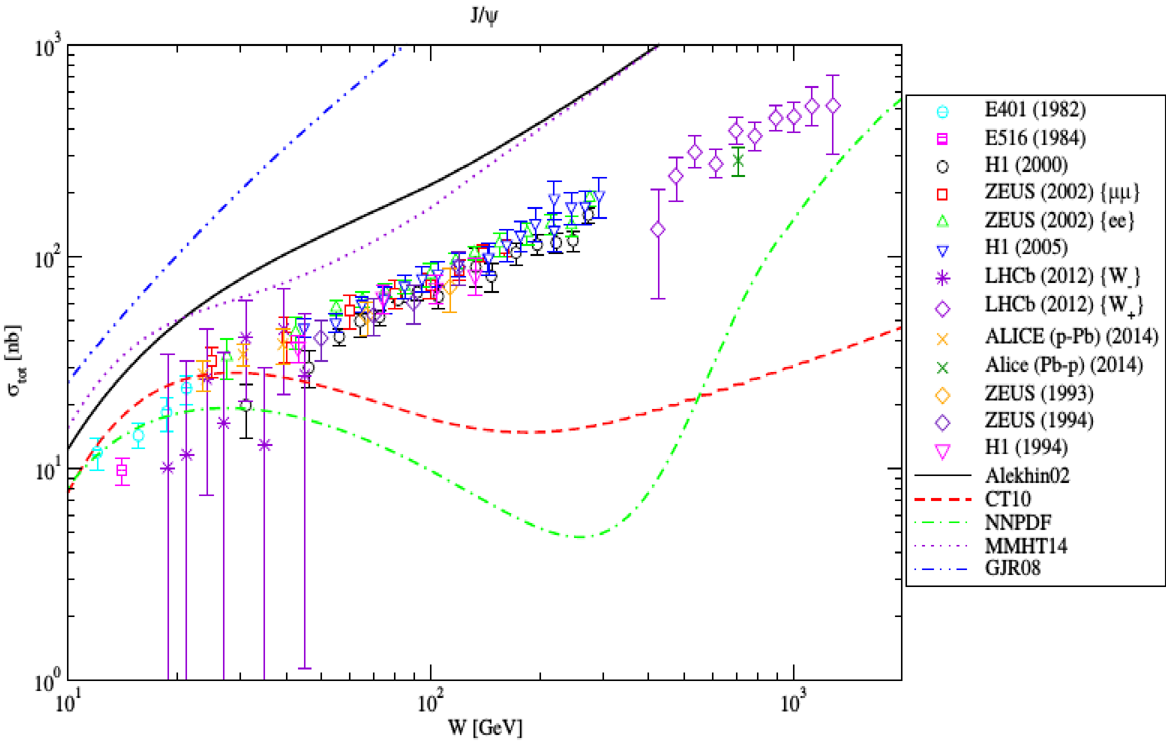

VPG, Martins, Sauter, EPJC76 (2016)

Diffractive vector meson photoproduction in UPHIC: Probing the gluon distribution

$$\left.\frac{d\sigma^{\gamma h \to Vh}}{dt}\right|_{t=0} = \mathcal{N}\frac{\pi^3\Gamma_{e^+e^-}M_V^3}{48\alpha_{em}}\left[\frac{\alpha_s(\bar{Q}^2)}{\bar{Q}^4}xg_h(x,\bar{Q}^2)\right]^2$$

$$\bar{Q} = \xi M_V/2$$

Parametrization	ξ	J/ψ $\mathcal{N}$	χ^2/d.o.f.
Alekhin02	0.879	0.180	3.818
CT10	3.412	45.041	1.179
NNPDF	4.373	139.670	1.215
MMHT14	1.035	0.297	7.226
GJR08	2.202	0.755	11.740

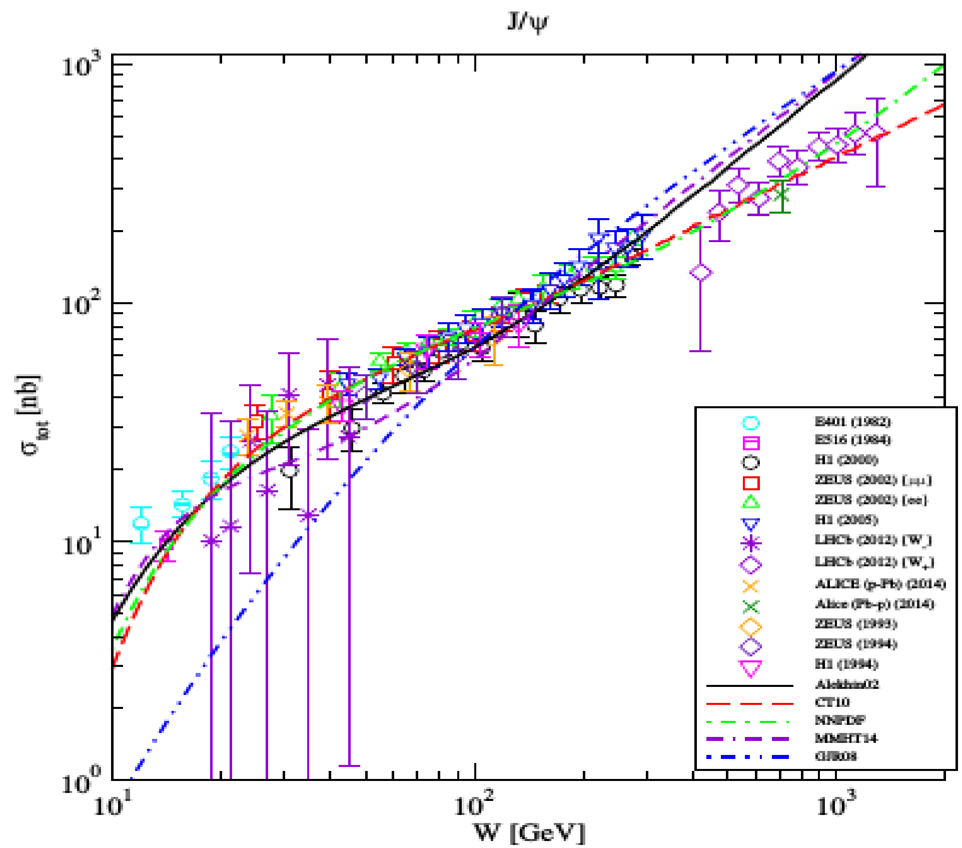

VPG, Martins, Sauter, EPJC76 (2016) 97

Diffractive vector meson photoproduction in UPHIC: Probing the gluon distribution

$$\left.\frac{d\sigma^{\gamma h\to Vh}}{dt}\right|_{t=0} = \mathcal{N}\frac{\pi^3\Gamma_{e^+e^-}M_V^3}{48\alpha_{em}}\left[\frac{\alpha_s(\bar{Q}^2)}{\bar{Q}^4}xg_h(x,\bar{Q}^2)\right]^2$$

$$\bar{Q} = \xi M_V/2$$

Parametrization	ξ	J/ψ $\mathcal{N}$	χ^2/d.o.f.
Alekhin02	0.879	0.180	3.818
CT10	3.412	45.041	1.179
NNPDF	4.373	139.670	1.215
MMHT14	1.035	0.297	7.226
GJR08	2.202	0.755	11.740

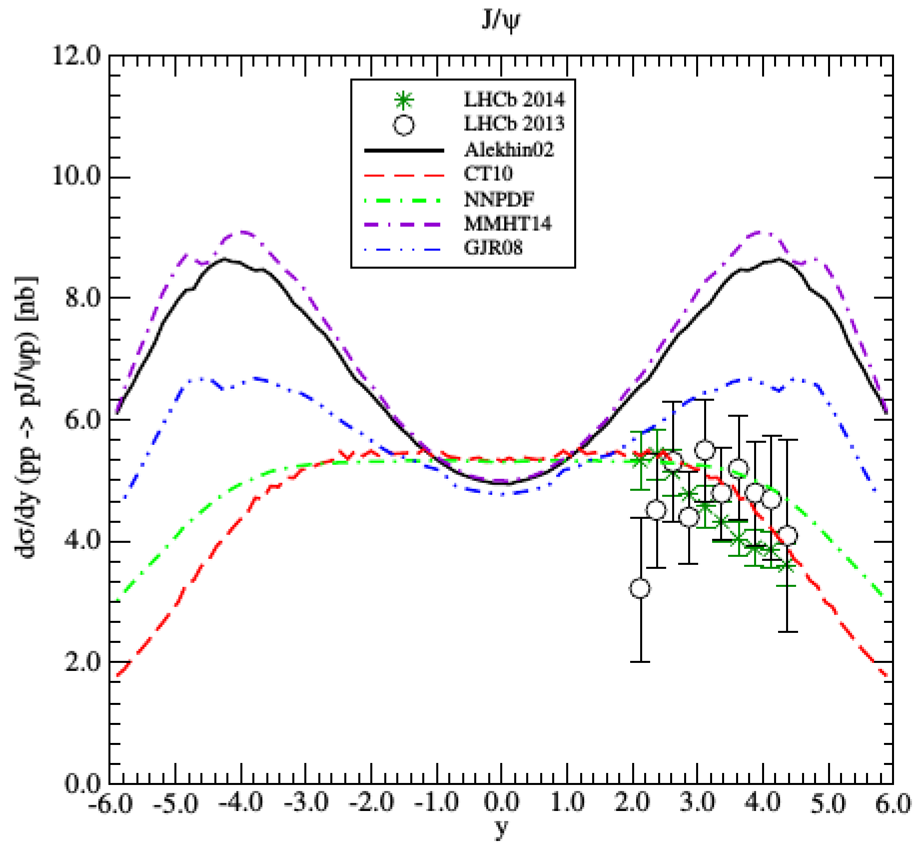

VPG, Martins, Sauter, EPJC76 (2016) 97

Diffractive vector meson photoproduction in UPHIC: Probing the gluon distribution

Parametrization	J/ψ ξ	J/ψ $\mathcal{N}$	J/ψ χ^2/d.o.f.	$\Psi(2S)$ ξ	$\Psi(2S)$ $\mathcal{N}$	$\Psi(2S)$ χ^2/d.o.f.	Υ ξ	Υ $\mathcal{N}$	Υ χ^2/d.o.f.
Alekhin02	0.879	0.180	3.818	0.816	0.133	1.520	$8.488 \cdot 10^{-2}$	$1.087 \cdot 10^{-4}$	0.624
CT10	3.412	45.041	1.179	3.783	59.331	1.682	0.614	0.188	0.312
NNPDF	4.373	139.670	1.215	5.064	208.837	1.871	0.939	1.063	0.312
MMHT14	1.035	0.297	7.226	0.641	0.101	1.220	0.135	3.690	1.820
GJR08	2.202	0.755	11.740	3.436	7.799	8.824	14.257	$1.428 \cdot 10^{3}$	3.707

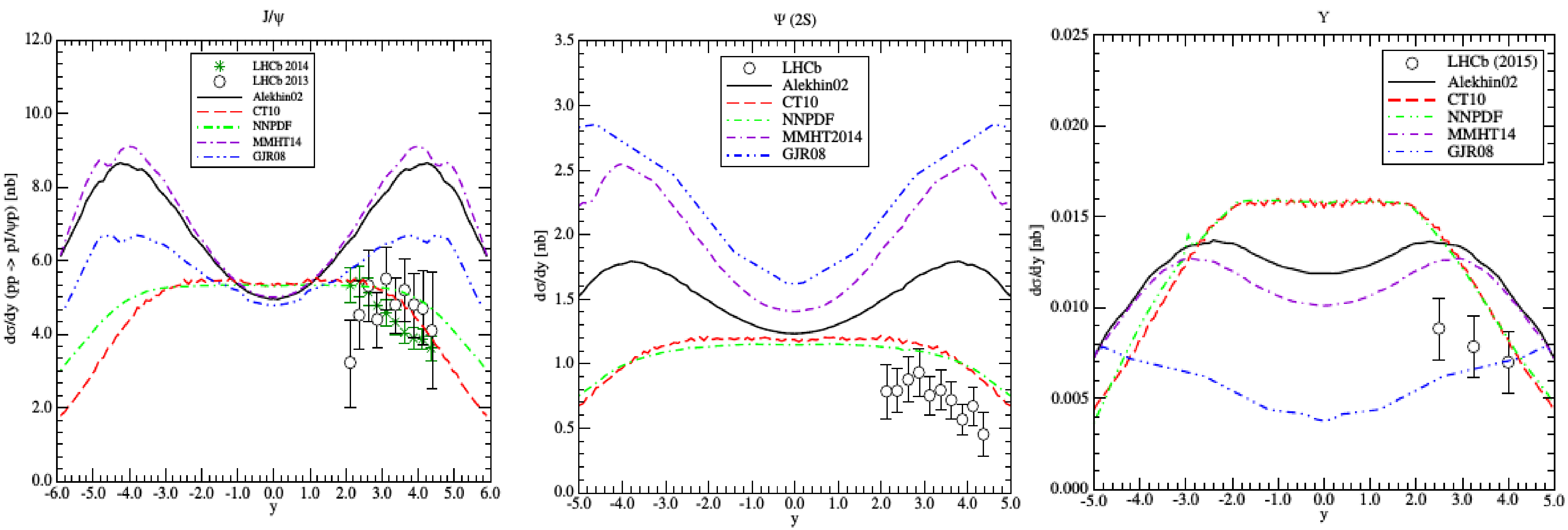

VPG, Martins, Sauter, EPJC76 (2016)

Diffractive vector meson photoproduction in UPHIC: Probing the gluon distribution

	J/ψ			$\Psi(2S)$			Υ		
Parametrization	ξ	$\mathcal{N}$	χ^2/d.o.f.	ξ	$\mathcal{N}$	χ^2/d.o.f.	ξ	$\mathcal{N}$	χ^2/d.o.f.
Alekhin02	0.879	0.180	3.818	0.816	0.133	1.520	$8.488 \cdot 10^{-2}$	$1.087 \cdot 10^{-4}$	0.624
CT10	3.412	45.041	1.179	3.783	59.331	1.682	0.614	0.188	0.312
NNPDF	4.373	139.670	1.215	5.064	208.837	1.871	0.939	1.063	0.312
MMHT14	1.035	0.297	7.226	0.641	0.101	1.220	0.135	3.690	1.820
GJR08	2.202	0.755	11.740	3.436	7.799	8.824	14.257	$1.428 \cdot 10^{3}$	3.707

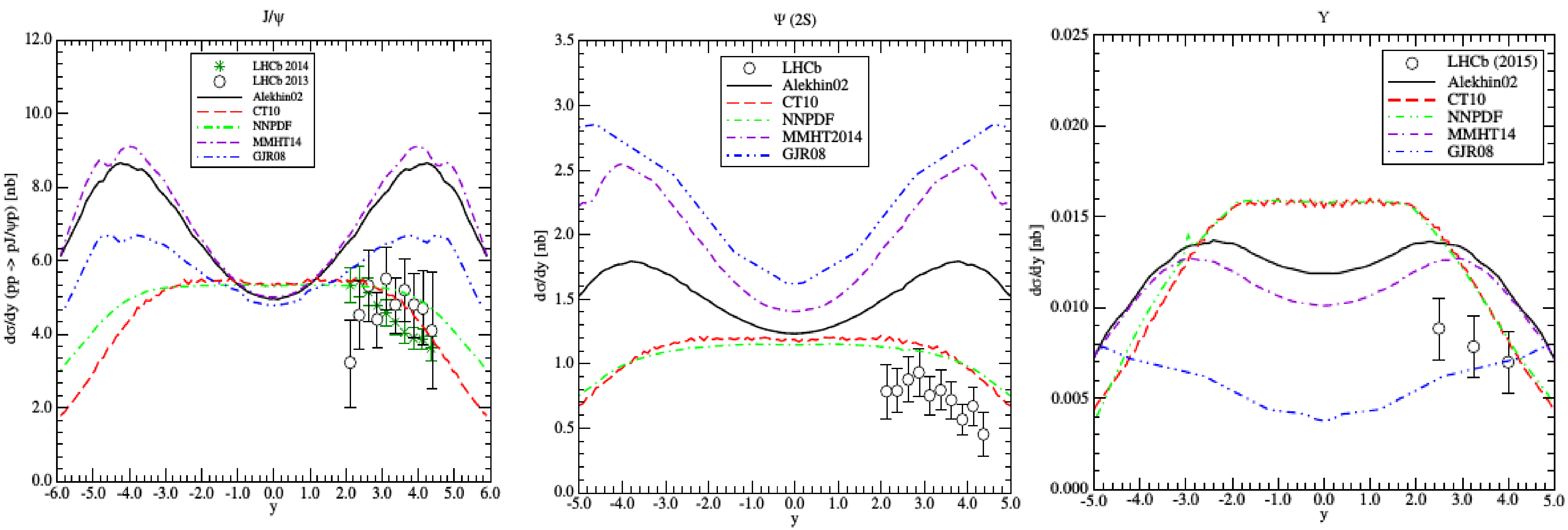

Description of data in the LL(1/x) approach is not possible using xg derived in the PDF global analysis !

Diffractive vector meson photoproduction in UPHIC: Probing the gluon distribution

Possible interpretations:

Diffractive vector meson photoproduction in UPHIC: Probing the gluon distribution

Possible interpretations:

1-) We need to take into account the NLO corrections to the LL(1/x) approach.

- Recent studies demonstrated that these corrections are huge (not yet under theoretical control).

Diffractive vector meson photoproduction in UPHIC: Probing the gluon distribution

Possible interpretations:

1-) We need to take into account the NLO corrections to the LL(1/x) approach.

- Recent studies demonstrated that these corrections are huge (not yet under theoretical control).

2-) New dynamical effects (beyond DGLAP!) are present at the large energies (small values of x) probed by the diffractive photoproduction of vector mesons at the LHC.

- We should to use another approach to describe the process !

QCD dynamics at high energies

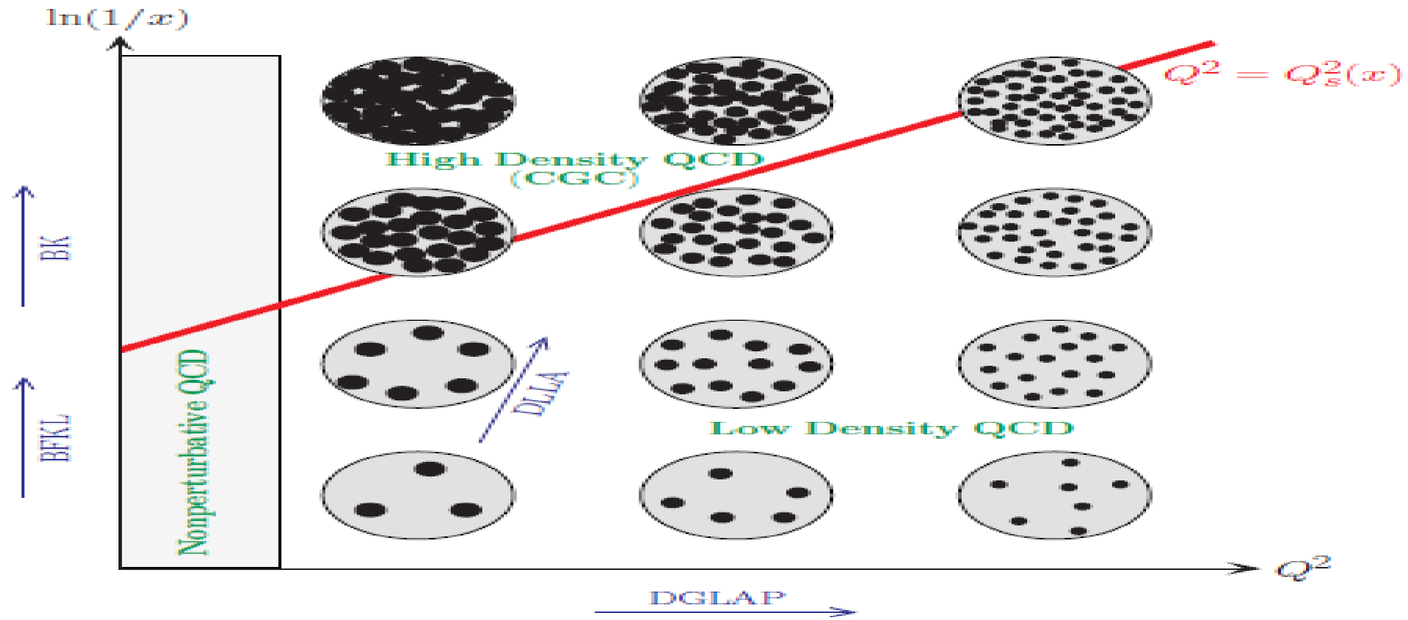

- Linear QCD Evolution equations predict a power growth of gluon distribution at small -x that implies the violation of unitarity;

QCD dynamics at high energies

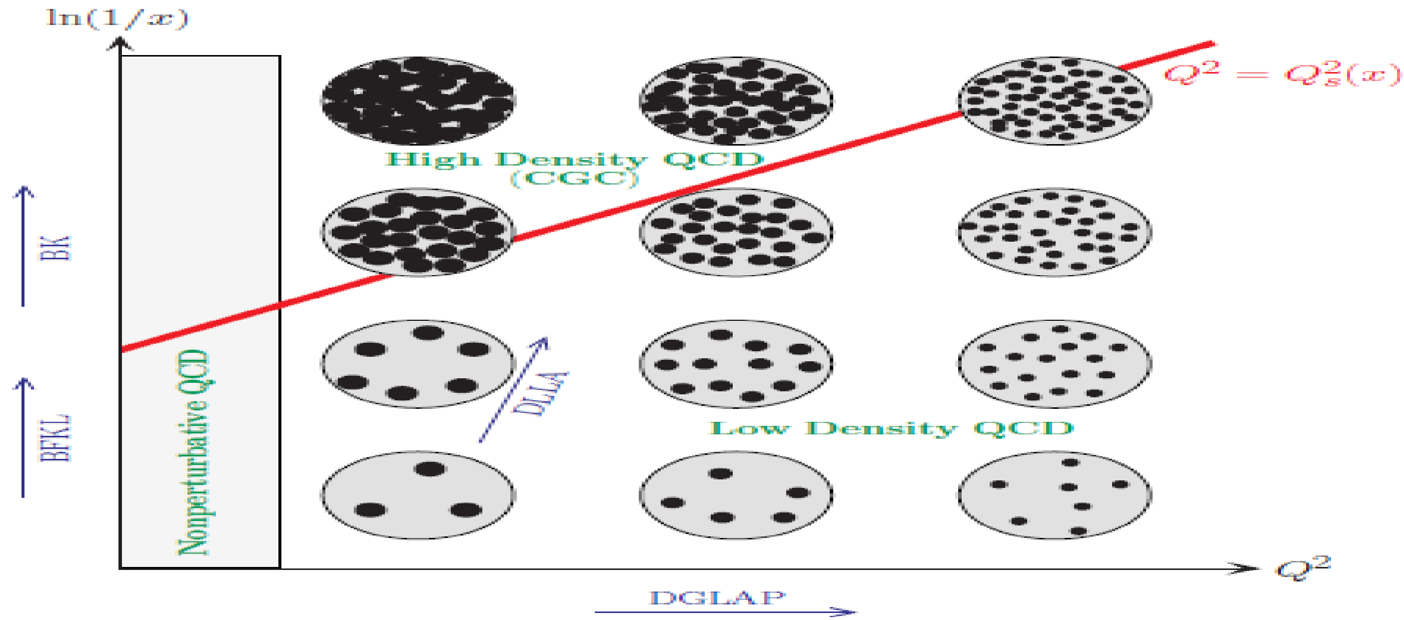

- Linear QCD Evolution equations predict a power growth of gluon distribution at small −x that implies the violation of unitarity;
- Number of gluons in the hadron becomes só large that gluon recombine. Nonlinear effects should be taken into account.

QCD dynamics at high energies

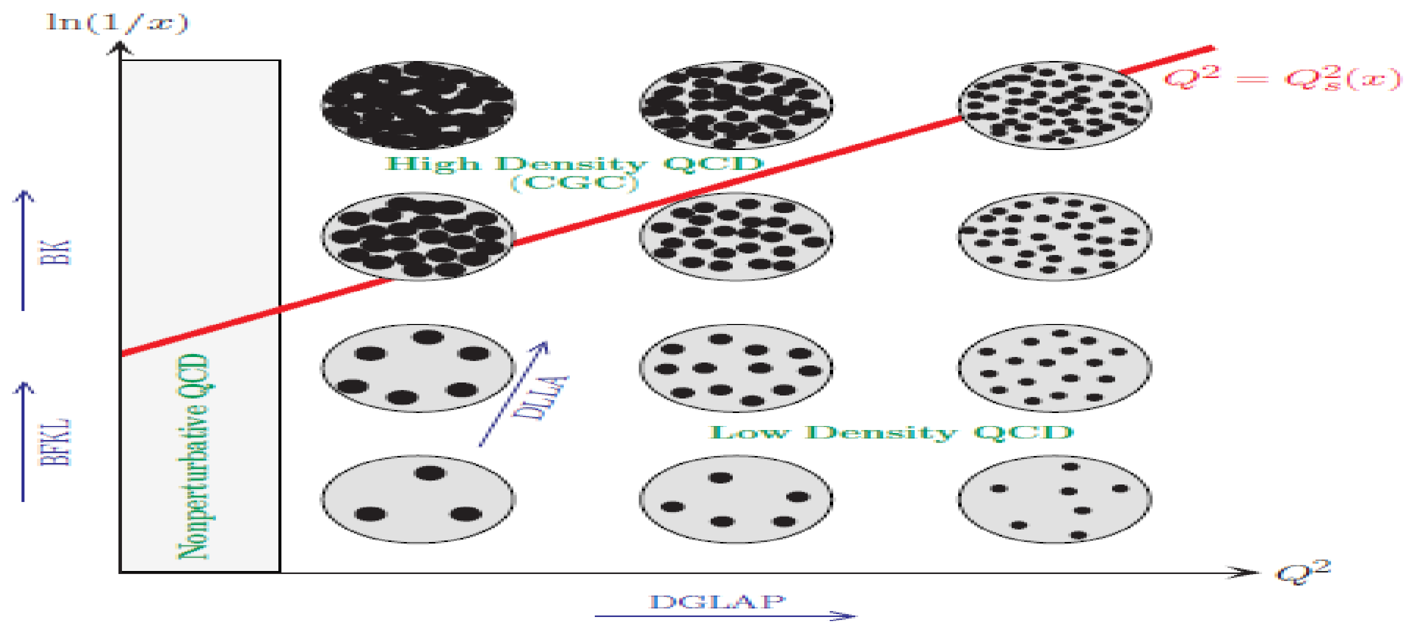

- Linear QCD Evolution equations predict a power growth of gluon distribution at small −x that implies the violation of unitarity;
- Number of gluons in the hadron becomes só large that gluon recombine. Nonlinear effects should be taken into account.
- Saturation scale Qs [proportional to $(1/x)^{\lambda/2} A^{\beta}$] defines the onset of nonlinear QCD dynamics (Gluon saturation effects).

QCD dynamics at high energies

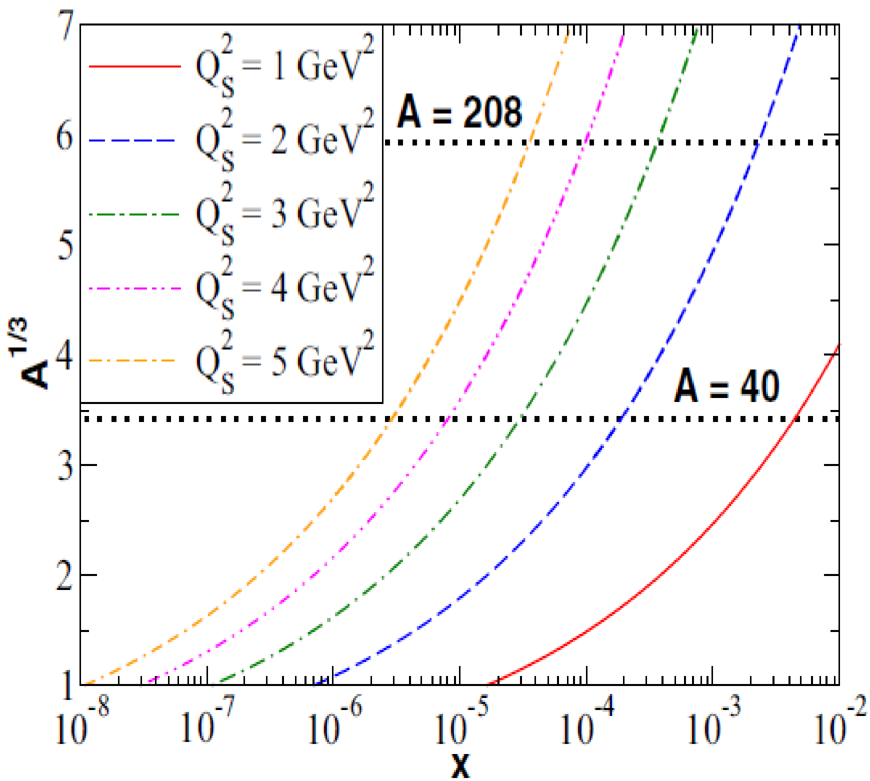

- Saturation scale Qs [proportional to $(1/x)^{\lambda/2}A^{\beta}$] defines the onset of nonlinear QCD dynamics (Gluon saturation effects);
- Nuclei are an efficient amplifier of the gluon saturation effects.

Diffractive vector meson photoproduction in UPHIC: Color Dipole Formalism

$$\frac{d\sigma\left[h_1 + h_2 \to h_1 \otimes V \otimes h_2\right]}{d^2b dy} = \left[\omega N_{h_1}(\omega, b)\, \sigma_{\gamma h_2 \to V \otimes h_2}(\omega)\right]_{\omega_L} + \left[\omega N_{h_2}(\omega, b)\, \sigma_{\gamma h_1 \to V \otimes h_1}(\omega)\right]_{\omega_R}$$

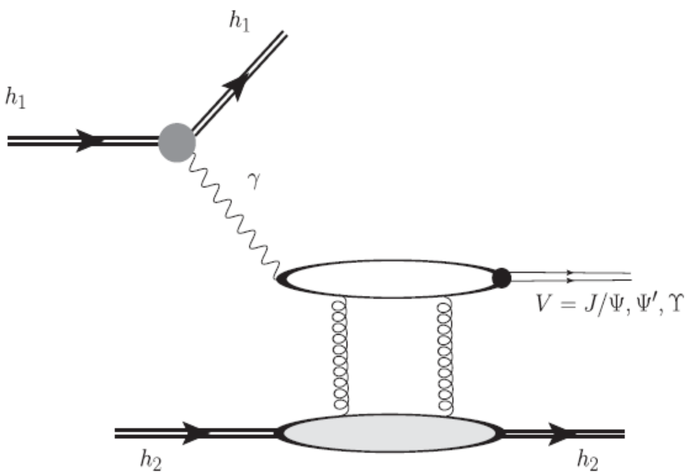

$$\sigma(\gamma h \to V h) = \int_{-\infty}^{0} \frac{d\sigma}{dt}\, dt = \frac{1}{16\pi} \int_{-\infty}^{0} |\mathcal{A}_T^{\gamma h \to V h}(x, \Delta)|^2\, dt$$

$$\mathcal{A}_T^{\gamma h \to V h}(x, \Delta) = i \int dz\, d^2\boldsymbol{r}\, d^2\boldsymbol{b}_h e^{-i[\boldsymbol{b}_h - (1-z)\boldsymbol{r}].\boldsymbol{\Delta}}\ (\Psi^{V*}\Psi)_T\ 2\mathcal{N}_h(x, \boldsymbol{r}, \boldsymbol{b}_h)$$

[a] VPG, Machado, EPJC 40, 519 (2005)

Diffractive vector meson photoproduction in UPHIC: Color Dipole Formalism

$$\frac{d\sigma\,[h_1 + h_2 \to h_1 \otimes V \otimes h_2]}{d^2b dy} = \left[\omega N_{h_1}(\omega, b)\,\sigma_{\gamma h_2 \to V \otimes h_2}(\omega)\right]_{\omega_L} + \left[\omega N_{h_2}(\omega, b)\,\sigma_{\gamma h_1 \to V \otimes h_1}(\omega)\right]_{\omega_R}$$

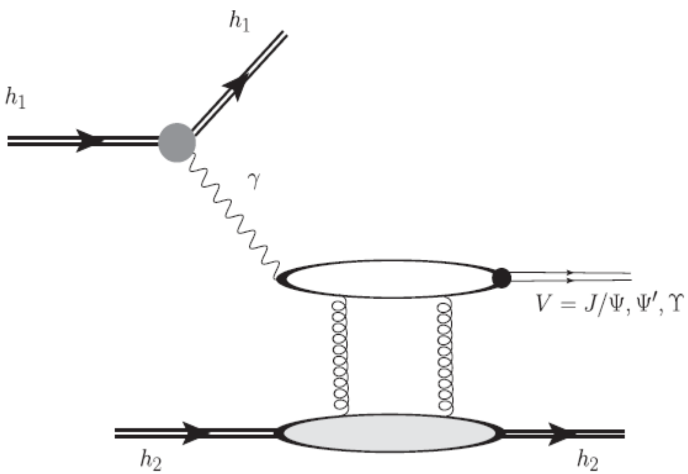

$$\sigma(\gamma h \to V h) = \int_{-\infty}^{0} \frac{d\sigma}{dt}\,dt = \frac{1}{16\pi}\int_{-\infty}^{0} |\mathcal{A}_T^{\gamma h \to V h}(x, \Delta)|^2\,dt$$

$$\mathcal{A}_T^{\gamma h \to V h}(x, \Delta) = i \int dz\, d^2\boldsymbol{r}\, d^2\boldsymbol{b}_h e^{-i[\boldsymbol{b}_h - (1-z)\boldsymbol{r}].\boldsymbol{\Delta}}\, \underbrace{(\Psi^{V*}\Psi)_T}\, 2\mathcal{N}_h(x, \boldsymbol{r}, \boldsymbol{b}_h)$$

Overlap function for Vector Mesons

[a]VPG, Machado, EPJC 40, 519 (2005)

Diffractive vector meson photoproduction in UPHIC: Color Dipole Formalism

$$\frac{d\sigma\,[h_1 + h_2 \rightarrow h_1 \otimes V \otimes h_2]}{d^2b dy} = \left[\omega N_{h_1}(\omega, b)\, \sigma_{\gamma h_2 \rightarrow V \otimes h_2}(\omega)\right]_{\omega_L} + \left[\omega N_{h_2}(\omega, b)\, \sigma_{\gamma h_1 \rightarrow V \otimes h_1}(\omega)\right]_{\omega_R}$$

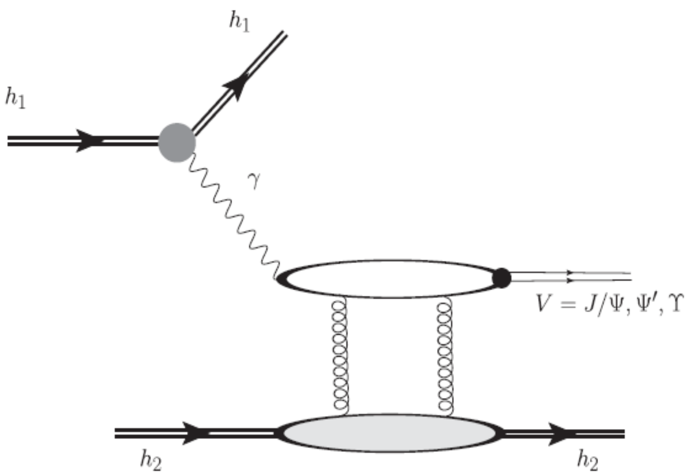

$$\sigma(\gamma h \rightarrow V h) = \int_{-\infty}^{0} \frac{d\sigma}{dt}\, dt = \frac{1}{16\pi} \int_{-\infty}^{0} |\mathcal{A}_T^{\gamma h \rightarrow V h}(x, \Delta)|^2\, dt$$

$$\mathcal{A}_T^{\gamma h \rightarrow V h}(x, \Delta) = i \int dz\, d^2\boldsymbol{r}\, d^2\boldsymbol{b}_h e^{-i[\boldsymbol{b}_h - (1-z)\boldsymbol{r}].\boldsymbol{\Delta}}\, (\Psi^{V*}\Psi)_T\; 2\mathcal{N}_h(x, \boldsymbol{r}, \boldsymbol{b}_h)$$

Forward dipole - hadron scattering amplitude: Determined by the QCD dynamics

[a]VPG, Machado, EPJC 40, 519 (2005)

Diffractive vector meson photoproduction in UPHIC: Color Glass Condensate Formalism

Dipole - proton scattering amplitude:

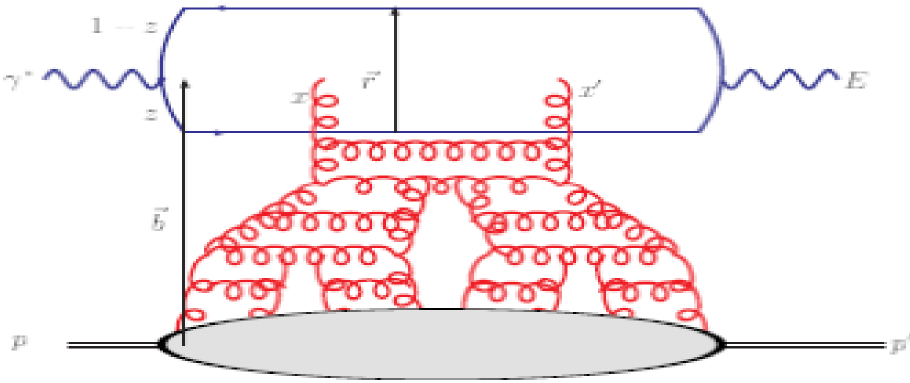

- bCGC :

$$\mathcal{N}^p(\hat{x}, \boldsymbol{r}, \boldsymbol{b}) = \begin{cases} \mathcal{N}_0\left(\frac{rQ_s(b)}{2}\right)^{2\left(\gamma_s + \frac{\ln(2/rQ_s(b))}{\kappa\lambda Y}\right)} & rQ_s(b) \leq 2 \\ 1 - e^{-A\ln^2(BrQ_s(b))} & rQ_s(b) > 2 \end{cases}$$

  - Proposed originally by Kowalski, Motyka and Watt (06)
  - Parameters of the model updated considering the high precision combined HERA data (Rezaeian, Schmidt, 13)

A unified description of combined inclusive HERA data & diffractive data in CGC

Rezaeian, Siddikov, Van de Klundert, Venugopalan, arXiv:1212.2974; Rezaeian, Schmidt, arXiv:1307.0825

The dipole scattering amplitude is the main ingredient with 3 or 4 free parameters fixed via a fit to the reduced cross–section.

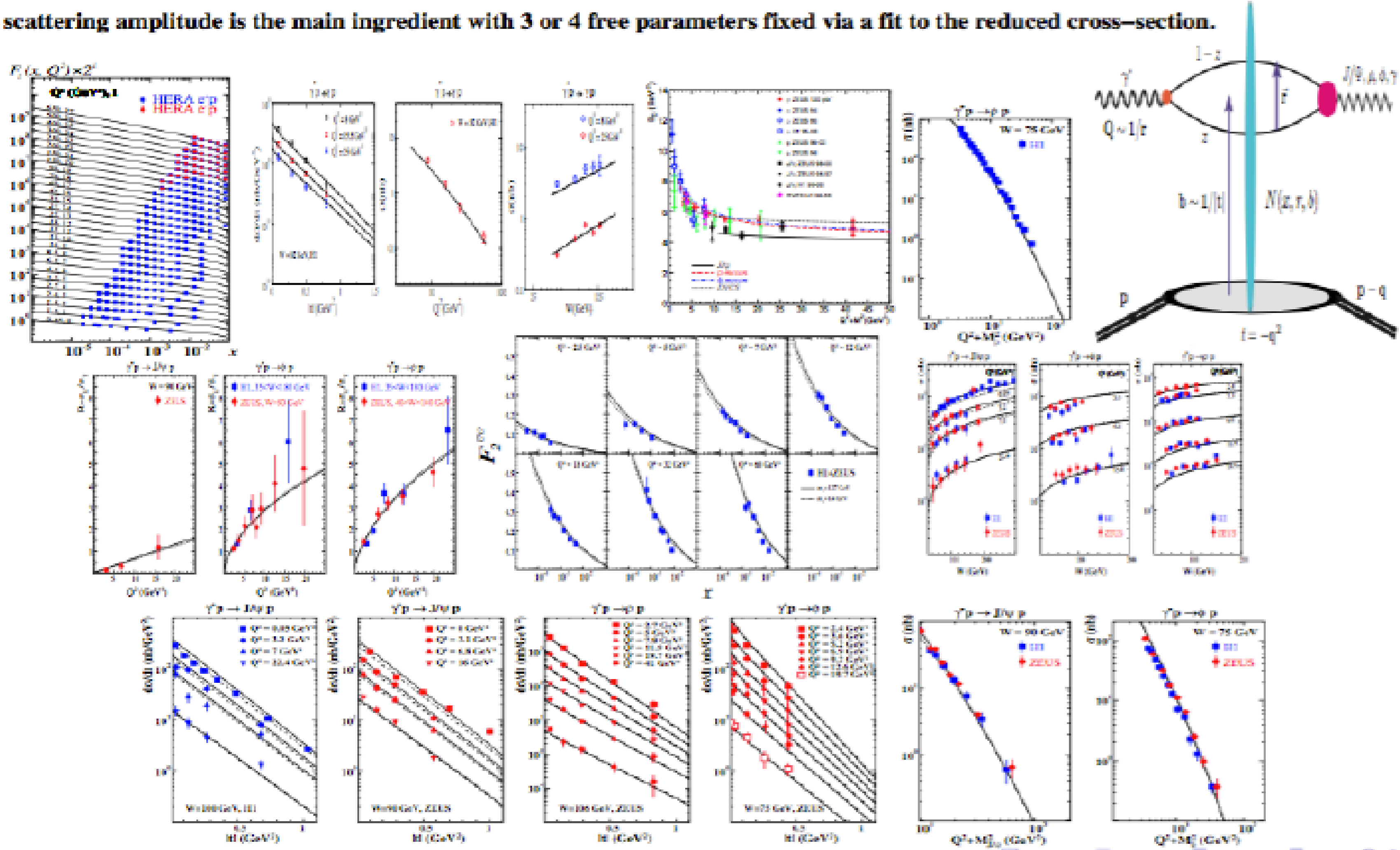

Rezaeian, INT workshop '17

Diffractive vector meson photoproduction in UPHIC: Color Dipole Formalism

$$\frac{d\sigma\,[h_1 + h_2 \to h_1 \otimes V \otimes h_2]}{d^2b dy} = [\omega N_{h_1}(\omega, b)\,\sigma_{\gamma h_2 \to V \otimes h_2}(\omega)]_{\omega_L} + [\omega N_{h_2}(\omega, b)\,\sigma_{\gamma h_1 \to V \otimes h_1}(\omega)]_{\omega_R}$$

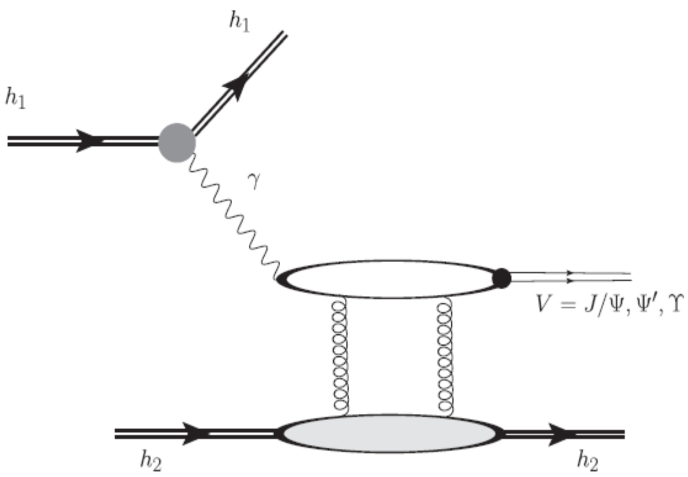

$$\sigma(\gamma h \to V h) = \int_{-\infty}^{0} \frac{d\sigma}{dt}\, dt = \frac{1}{16\pi} \int_{-\infty}^{0} |\mathcal{A}_T^{\gamma h \to V h}(x, \Delta)|^2\, dt$$

$$\mathcal{A}_T^{\gamma h \to V h}(x, \Delta) = i \int dz\, d^2\boldsymbol{r}\, d^2\boldsymbol{b}_h e^{-i[\boldsymbol{b}_h - (1-z)\boldsymbol{r}].\boldsymbol{\Delta}}\, (\Psi^{V*}\Psi)_T\, 2\mathcal{N}_h(x, \boldsymbol{r}, \boldsymbol{b}_h)$$

- Nucleus: $\mathcal{N}_A(x, \boldsymbol{r}, \boldsymbol{b}_A) = 1 - \exp\left[-\frac{1}{2}\sigma_{dp}(x, \boldsymbol{r}^2)\, T_A(\boldsymbol{b}_A)\right]$ ⇒ Sums all multiple elastic rescatterings of the dipole.

$$\sigma_{dp}(x, \boldsymbol{r}^2) = 2 \int d^2\boldsymbol{b}_p\, \mathcal{N}_p(x, \boldsymbol{r}, \boldsymbol{b}_p)$$

Diffractive vector meson photoproduction in UPHIC: Color Dipole Formalism

$$\frac{d\sigma\,[h_1 + h_2 \to h_1 \otimes V \otimes h_2]}{d^2b dy} = \left[\omega N_{h_1}(\omega, b)\, \sigma_{\gamma h_2 \to V \otimes h_2}(\omega)\right]_{\omega_L} + \left[\omega N_{h_2}(\omega, b)\, \sigma_{\gamma h_1 \to V \otimes h_1}(\omega)\right]_{\omega_R}$$

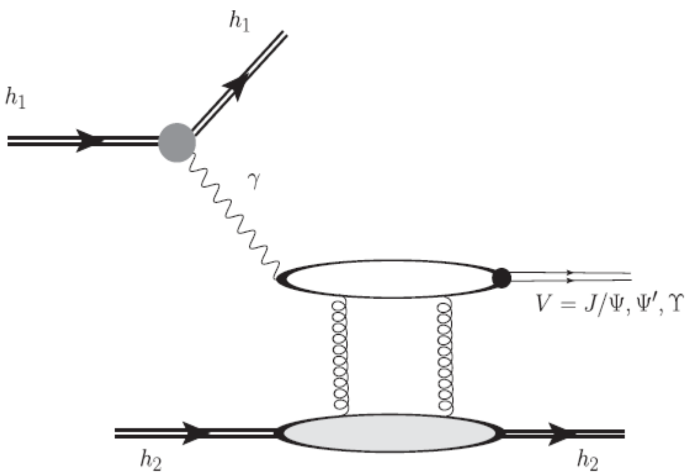

$$\sigma(\gamma h \to V h) = \int_{-\infty}^{0} \frac{d\sigma}{dt}\, dt = \frac{1}{16\pi} \int_{-\infty}^{0} |\mathcal{A}_T^{\gamma h \to V h}(x, \Delta)|^2\, dt$$

$$\mathcal{A}_T^{\gamma h \to V h}(x, \Delta) = i \int dz\, d^2\boldsymbol{r}\, d^2\boldsymbol{b}_h e^{-i[\boldsymbol{b}_h - (1-z)\boldsymbol{r}].\boldsymbol{\Delta}}\, (\Psi^{V*}\Psi)_T\; 2\mathcal{N}_h(x, \boldsymbol{r}, \boldsymbol{b}_h)$$

In the dipole picture, all free parameters have been constrained by HERA data. Predictions for UPHIC are parameter free!

Diffractive vector meson photoproduction in UPHIC: Impact of the gluon saturation effects

VPG, Spiering, Navarra, arXiv:1701.04340

Diffractive vector meson photoproduction in UPHIC: Impact of the gluon saturation effects

pp Collisions:

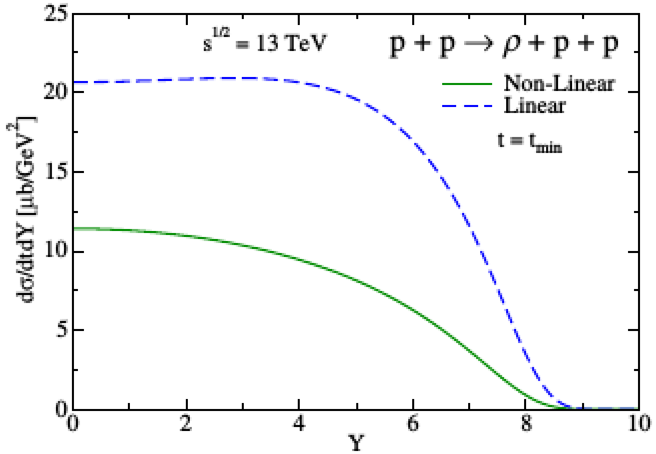

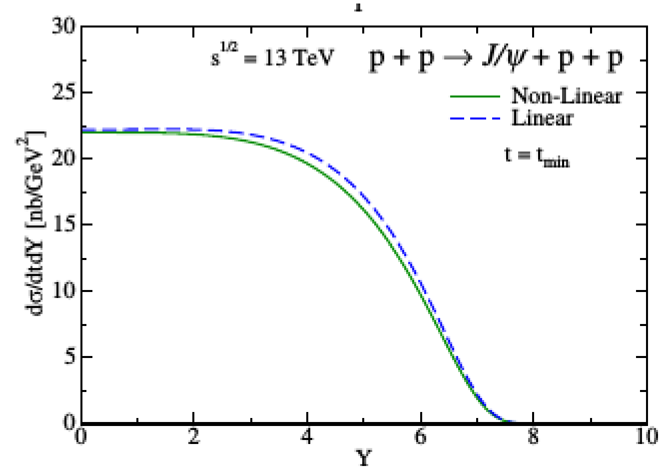

$$t_{min} = -m_N^2 M_V^4 / W^4$$

VPG, Spiering, Navarra, arXiv:1701.04340

Diffractive vector meson photoproduction in UPHIC: Impact of the gluon saturation effects

pp Collisions:

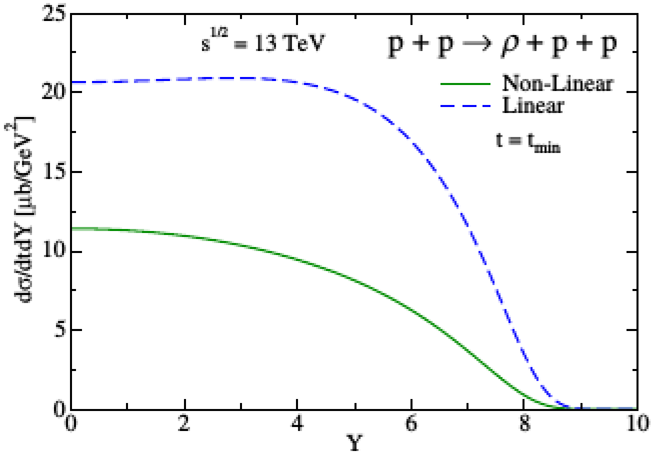

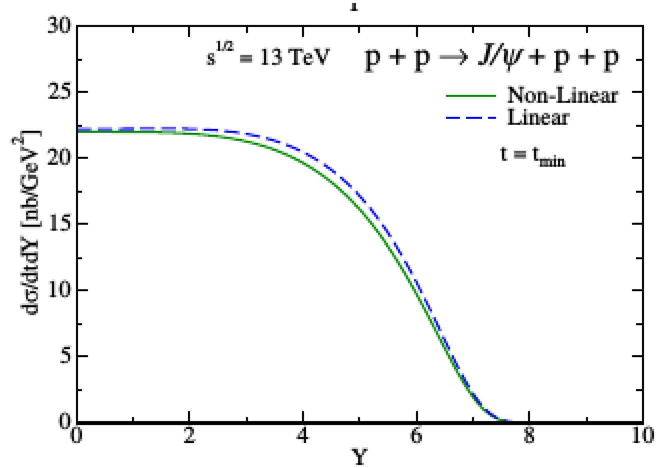

PbPb Collisions:

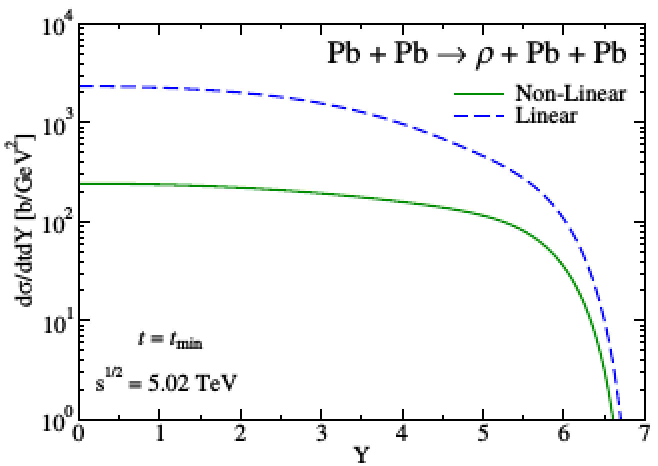

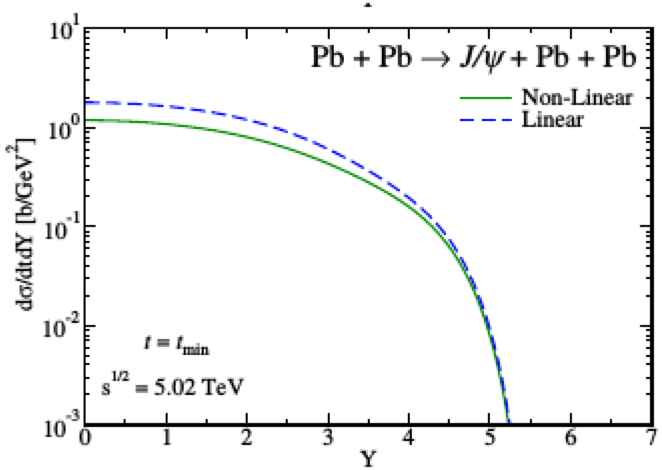

$t_{min} = -m_N^2 M_V^4 / W^4$

VPG, Spiering, Navarra, arXiv:1701.04340

Diffractive vector meson photoproduction in UPHIC: Impact of the gluon saturation effects

pp Collisions:

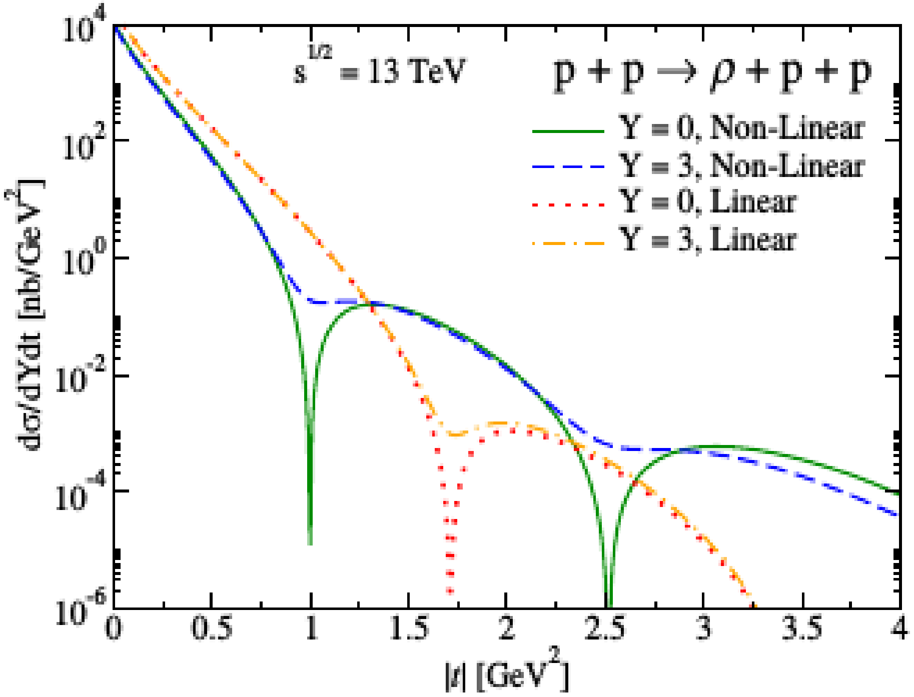

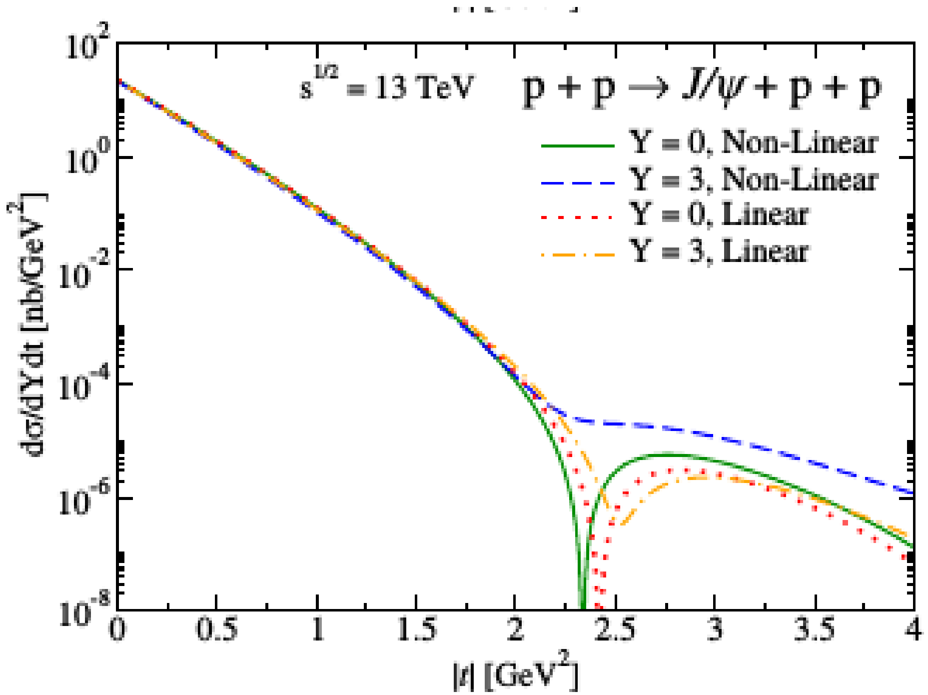

Linear model:

$$\mathcal{N}^p(x, \boldsymbol{r}, \boldsymbol{b}_p) = \mathcal{N}_0 \left(\frac{r\, Q_s(b_p)}{2}\right)^{2\left(\gamma_s + \frac{\ln(2/r\, Q_s(b_p))}{\kappa \lambda Y}\right)}$$

VPG, Spiering, Navarra, arXiv:1701.04340

Diffractive vector meson photoproduction in UPHIC: Impact of the gluon saturation effects

PbPb Collisions:

Coherent production:

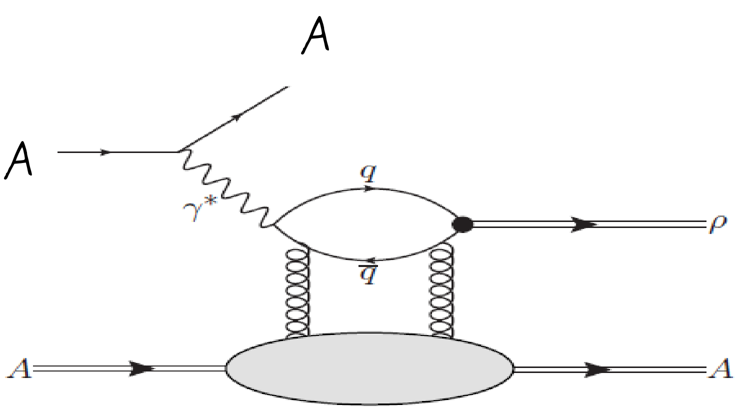

Incoherent production:

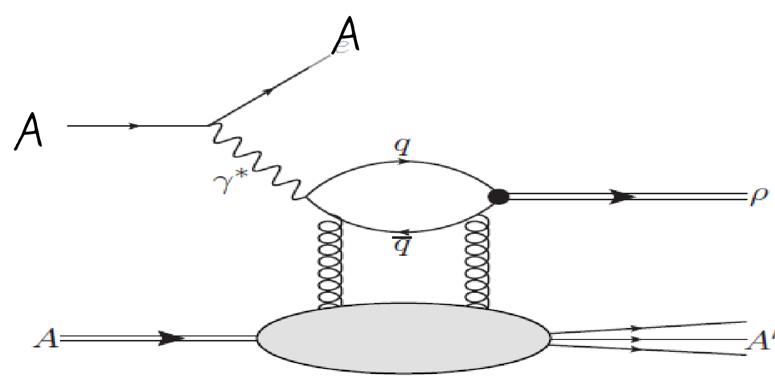

VPG, Spiering, Navarra, arXiv:1701.04340

Diffractive vector meson photoproduction in UPHIC: Impact of the gluon saturation effects

PbPb Collisions:

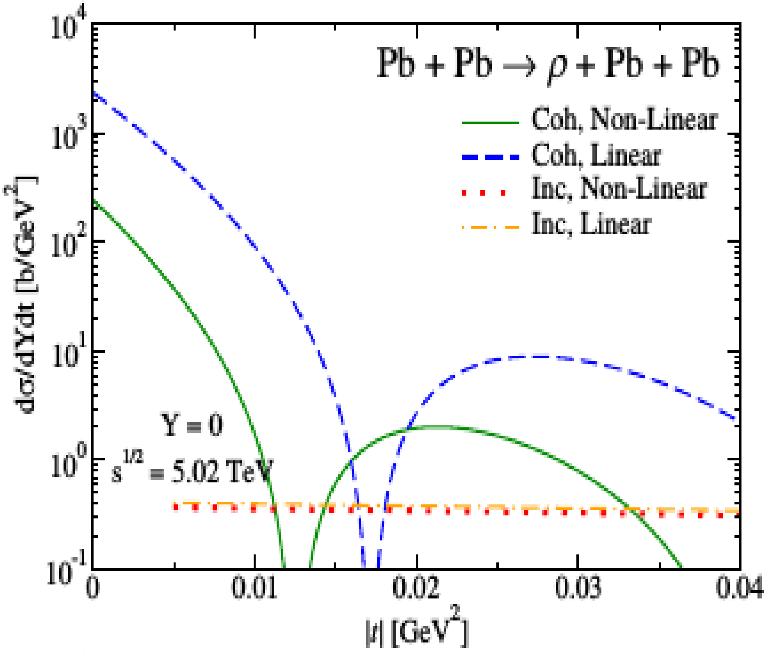

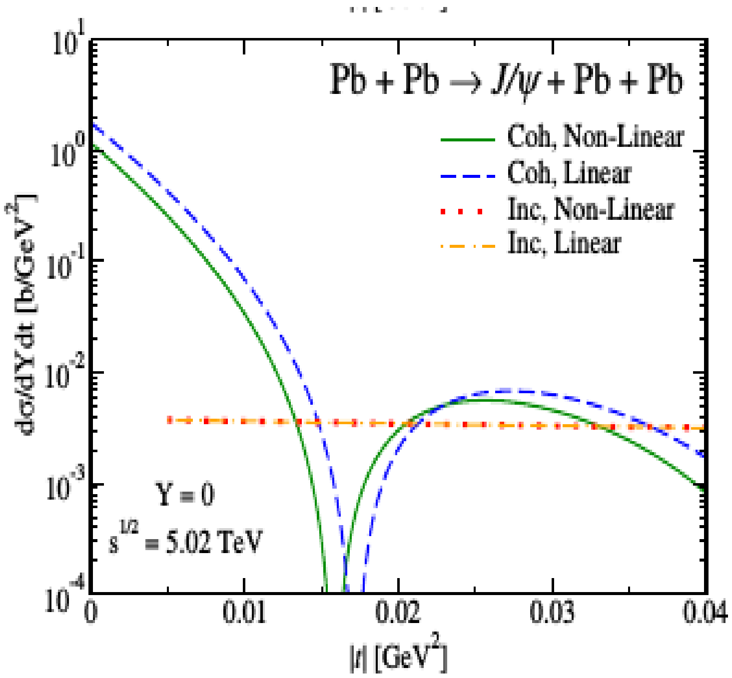

Linear model: $\mathcal{N}^A(x, r, \boldsymbol{b}_A) = \frac{1}{2}\sigma_{dp}(x, r) A T_A(\boldsymbol{b}_A)$

VPG, Spiering, Navarra, arXiv:1701.04340

Comparison with the LHC data

Comparison with the LHC data

Diffractive J/Psi photoproduction in pp collisions:

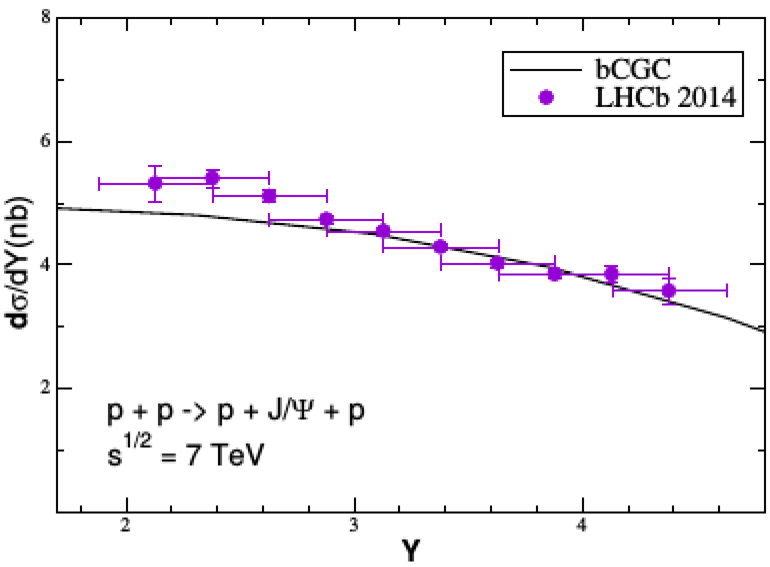

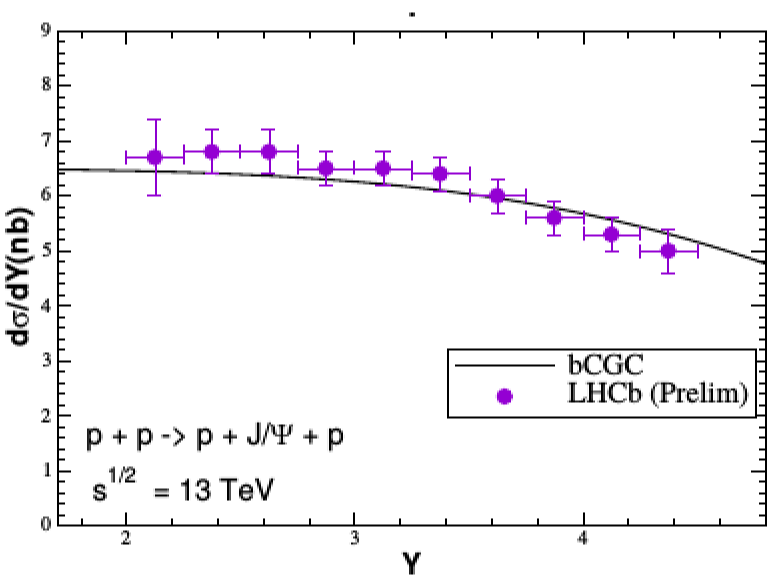

VPG, Moreira, Navarra, arXiv:1612.06254

Comparison with the LHC data

Diffractive Psi(2S) photoproduction in pp collisions:

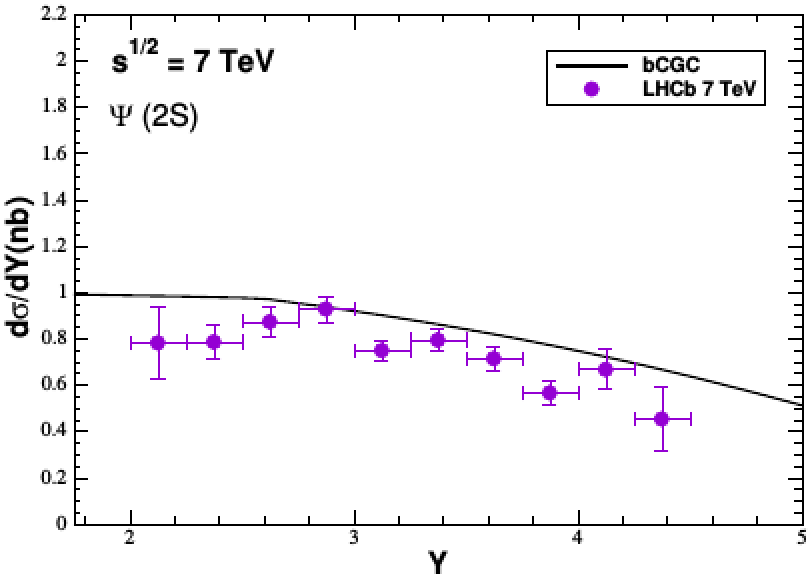

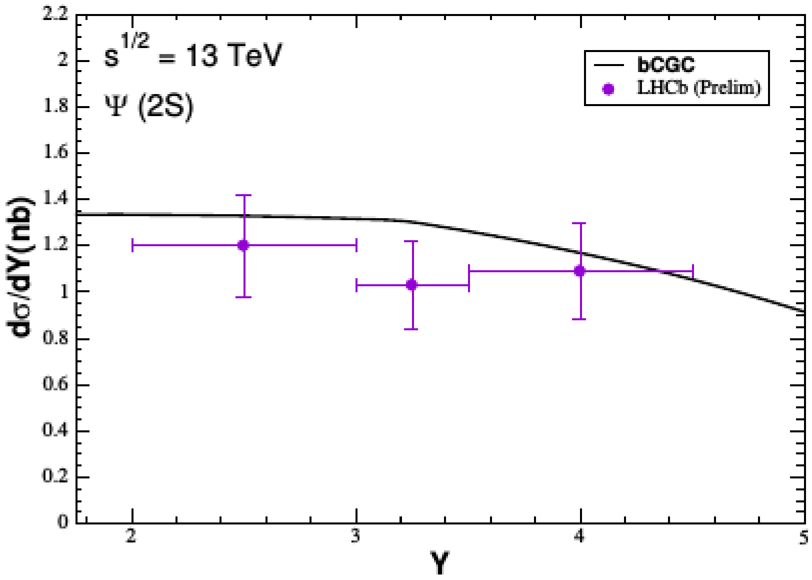

VPG, Moreira, Navarra, arXiv:1612.06254

Comparison with the LHC data

Diffractive Upsilon photoproduction in pp collisions:

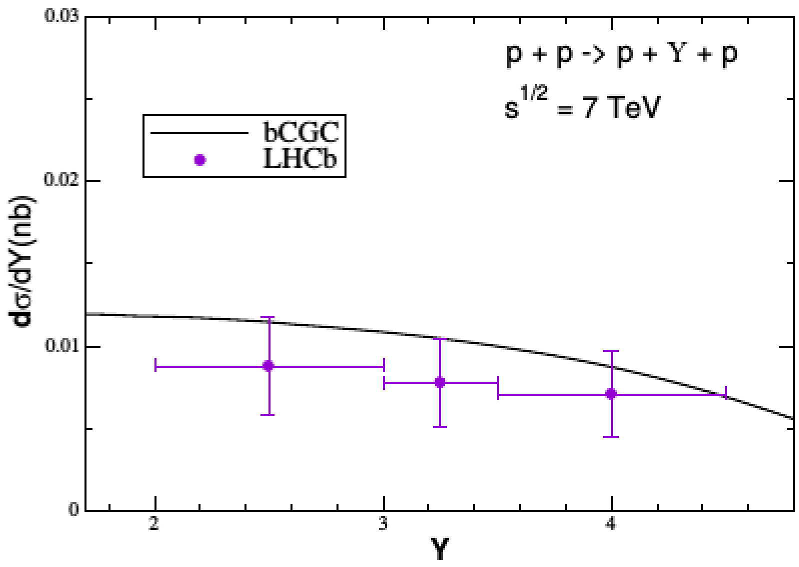

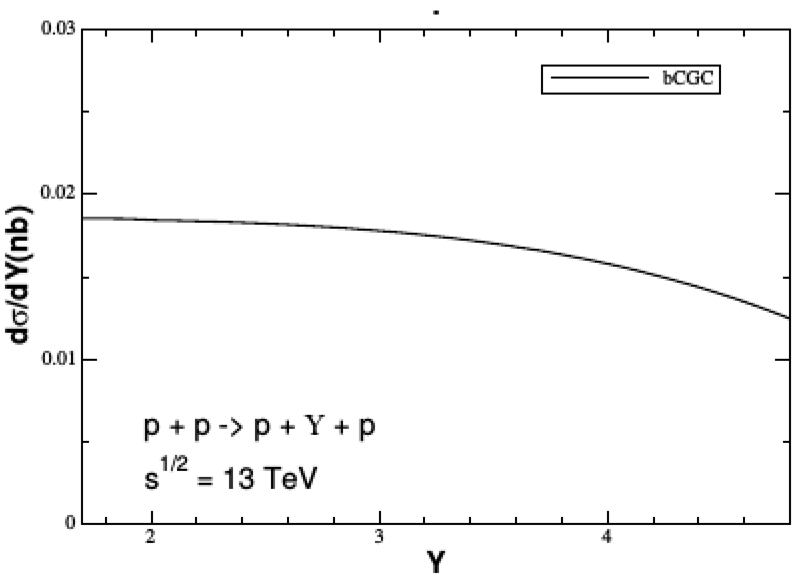

VPG, Moreira, Navarra, arXiv:1612.06254

Comparison with the LHC data

Energy dependence of the photon - proton cross section:

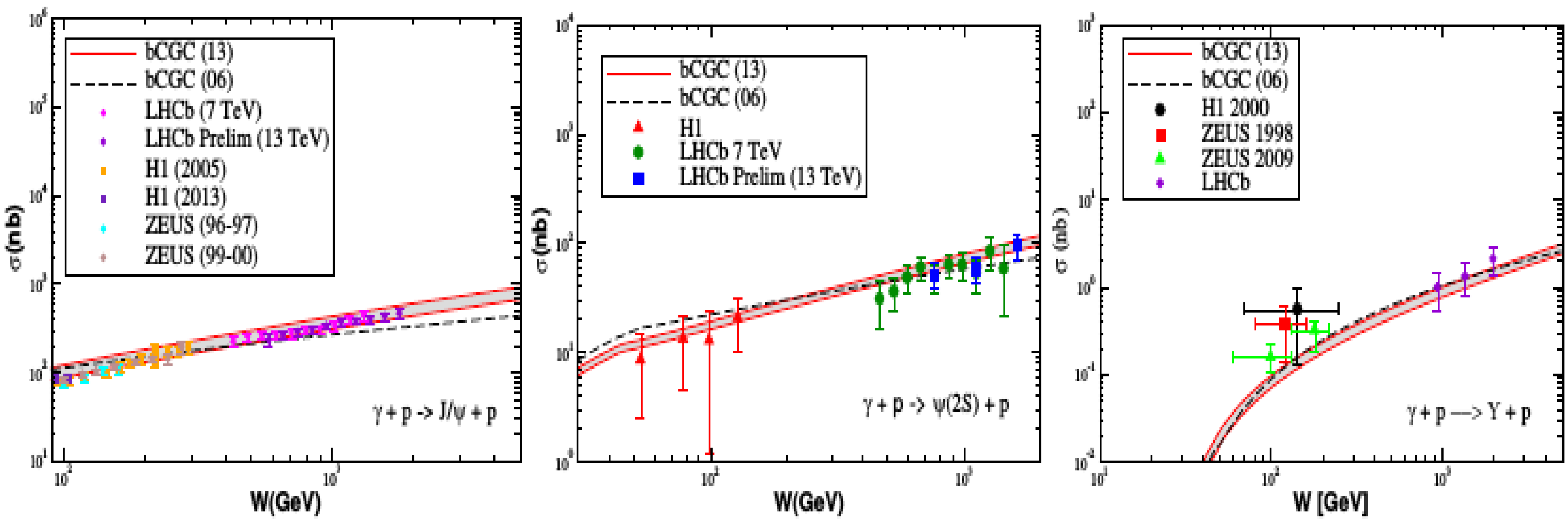

VPG, Moreira, Navarra, arXiv:1612.06254

Summary

Summary

- ✓ The diffractive vector meson photoproduction in photon – induced interactions at the LHC is an important probe of the QCD dynamics at high energies.
- ✓ The Run I data can be sucessfully described by the color dipole formalism taking into account the nonlinear effects in the QCD dynamics.
- ✓ The Run II data can be used to constrain the description of the dipole – hadron scattering amplitude and the vector meson wave function
- ✓ Complementary studies can be performed by analysis of the double vector meson production and the vector meson production associated to a leading neutron.

Summary

- ✓ The diffractive vector meson photoproduction in photon – induced interactions at the LHC is an important probe of the QCD dynamics at high energies.
- ✓ The Run I data can be sucessfully described by the color dipole formalism taking into account the nonlinear effects in the QCD dynamics.
- ✓ The Run II data can be used to constrain the description of the dipole – hadron scattering amplitude and the vector meson wave function
- ✓ Complementary studies can be performed by analysis of the double vector meson production and the vector meson production associated to a leading neutron.

Summary

- ✓ The diffractive vector meson photoproduction in photon – induced interactions at the LHC is an important probe of the QCD dynamics at high energies.
- ✓ The Run I data can be sucessfully described by the color dipole formalism taking into account the nonlinear effects in the QCD dynamics.
- ✓ The Run II data can be used to constrain the description of the dipole – hadron scattering amplitude and the vector meson wave function
- ✓ Complementary studies can be performed by analysis of the double vector meson production and the vector meson production associated to a leading neutron.

Summary

- ✓ The diffractive vector meson photoproduction in photon – induced interactions at the LHC is an important probe of the QCD dynamics at high energies.
- ✓ The Run I data can be sucessfully described by the color dipole formalism taking into account the nonlinear effects in the QCD dynamics.
- ✓ The Run II data can be used to constrain the description of the dipole – hadron scattering amplitude and the vector meson wave function
- ✓ Complementary studies can be performed by analysis of the double vector meson production and the vector meson production associated to a leading neutron.

Summary

- ✓ The diffractive vector meson photoproduction in photon – induced interactions at the LHC is an important probe of the QCD dynamics at high energies.
- ✓ The Run I data can be sucessfully described by the color dipole formalism taking into account the nonlinear effects in the QCD dynamics.
- ✓ The Run II data can be used to constrain the description of the dipole – hadron scattering amplitude and the vector meson wave function
- ✓ Complementary studies can be performed by analysis of the double vector meson production and the vector meson production associated to a leading neutron.

Thank you for your attention!

Extras

Comparison with the Run I data

- Diffractive J/Ψ photoproduction in hadronic collisions [a]

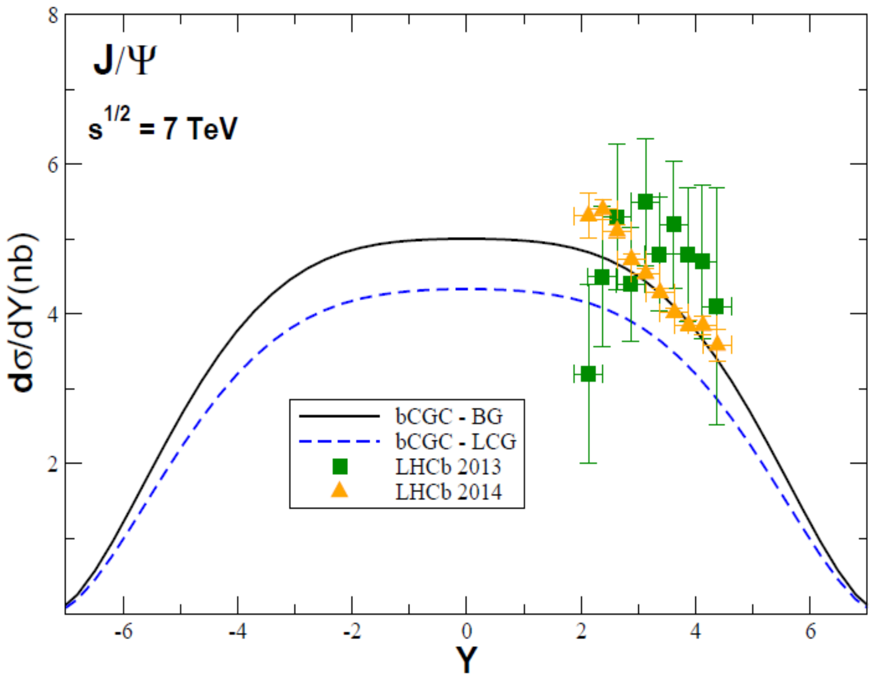

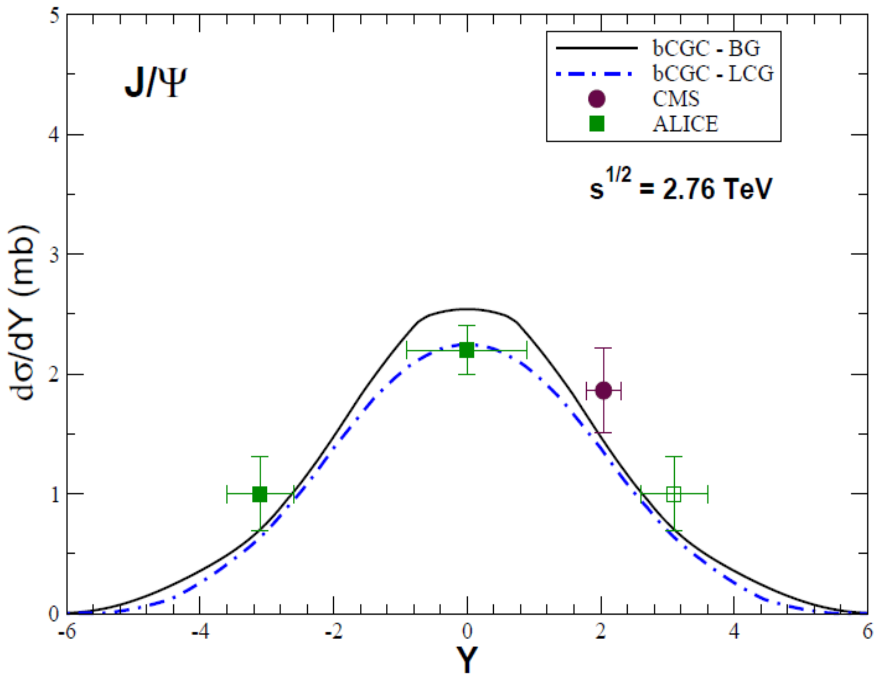

(a) VPG, Moreira, Navarra, PRC90, 015203 (2014)

Comparison with the Run I data

- Diffractive J/Ψ photoproduction in hadronic collisions [a]

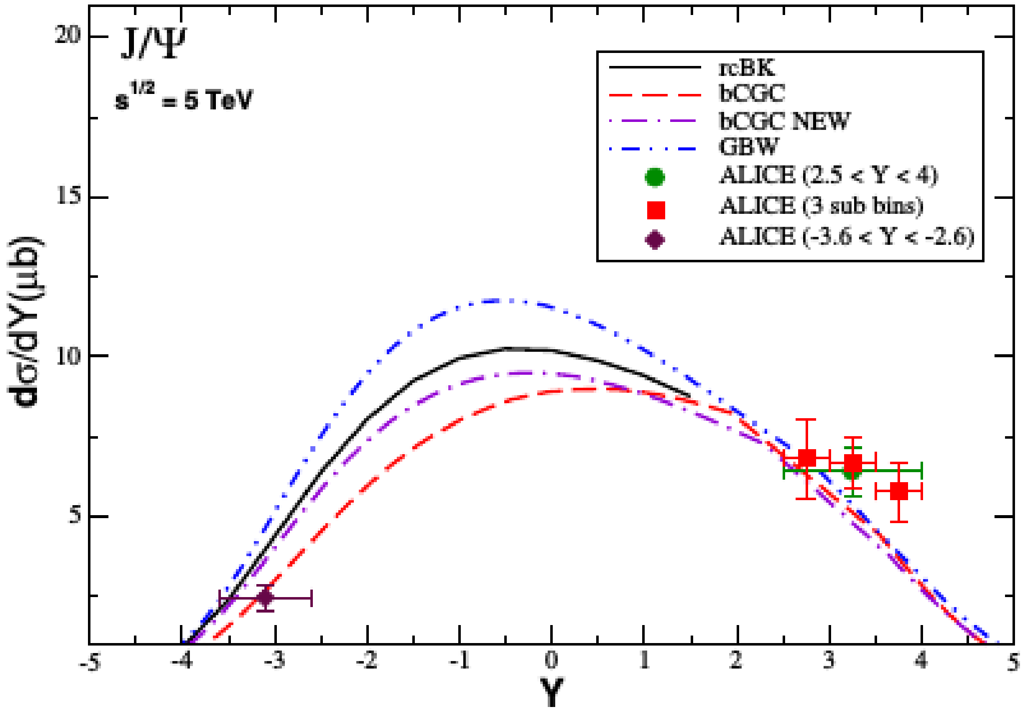

Comparison with the Run I data

- Diffractive ρ photoproduction in hadronic collisions [c]

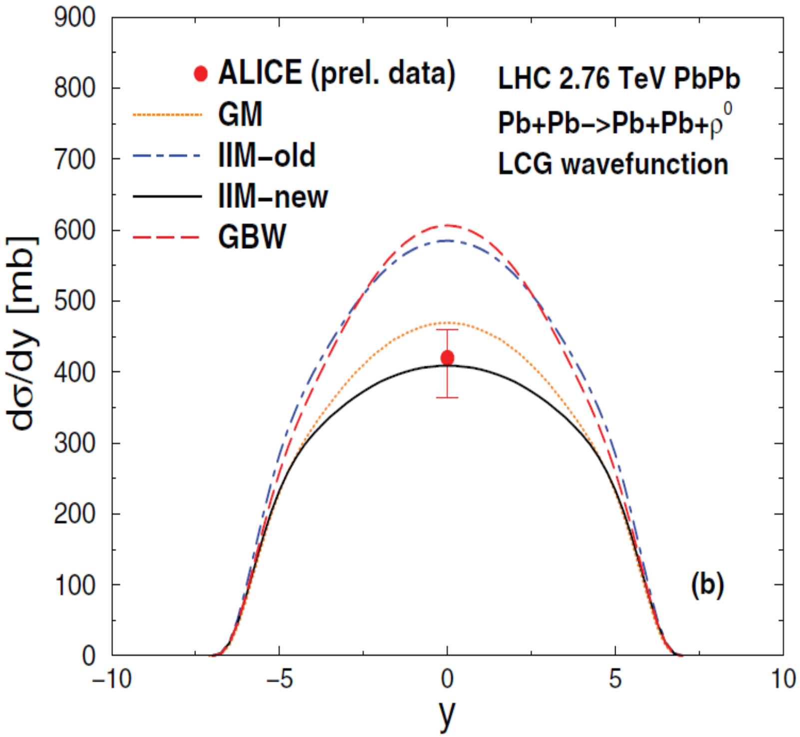

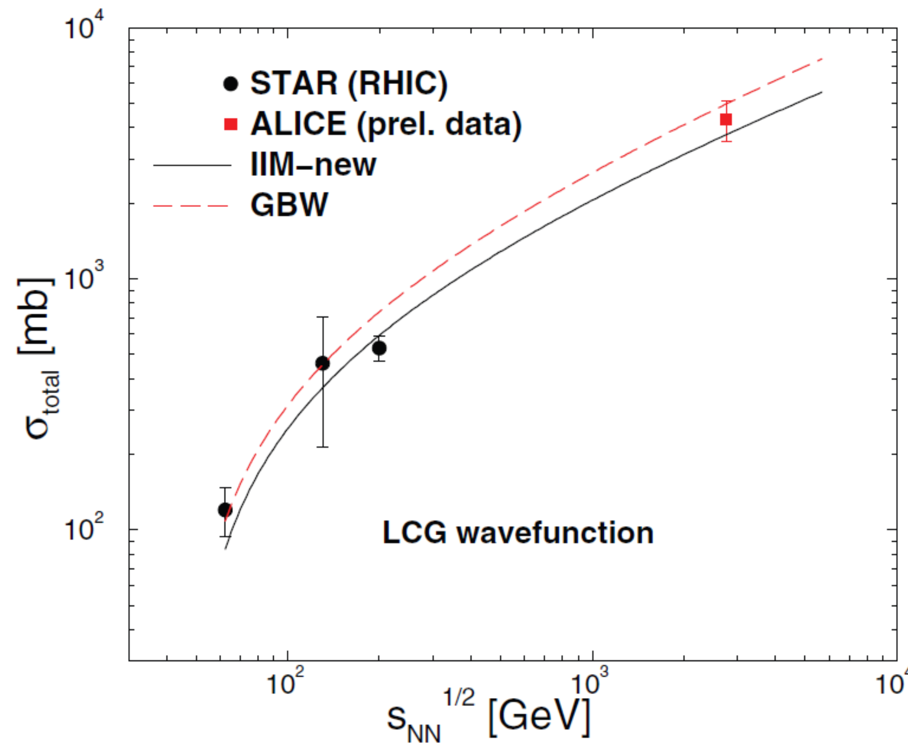

(c) VPG, Machado, EPJC 40, 519 (2005); PRC80, 054901 (2009); PRC84, 011902 (2011); Machado, dos Santos, PRC91, 025203 (2015)

Comparison with the Run I data

- Diffractive Υ photoproduction in hadronic collisions [b]

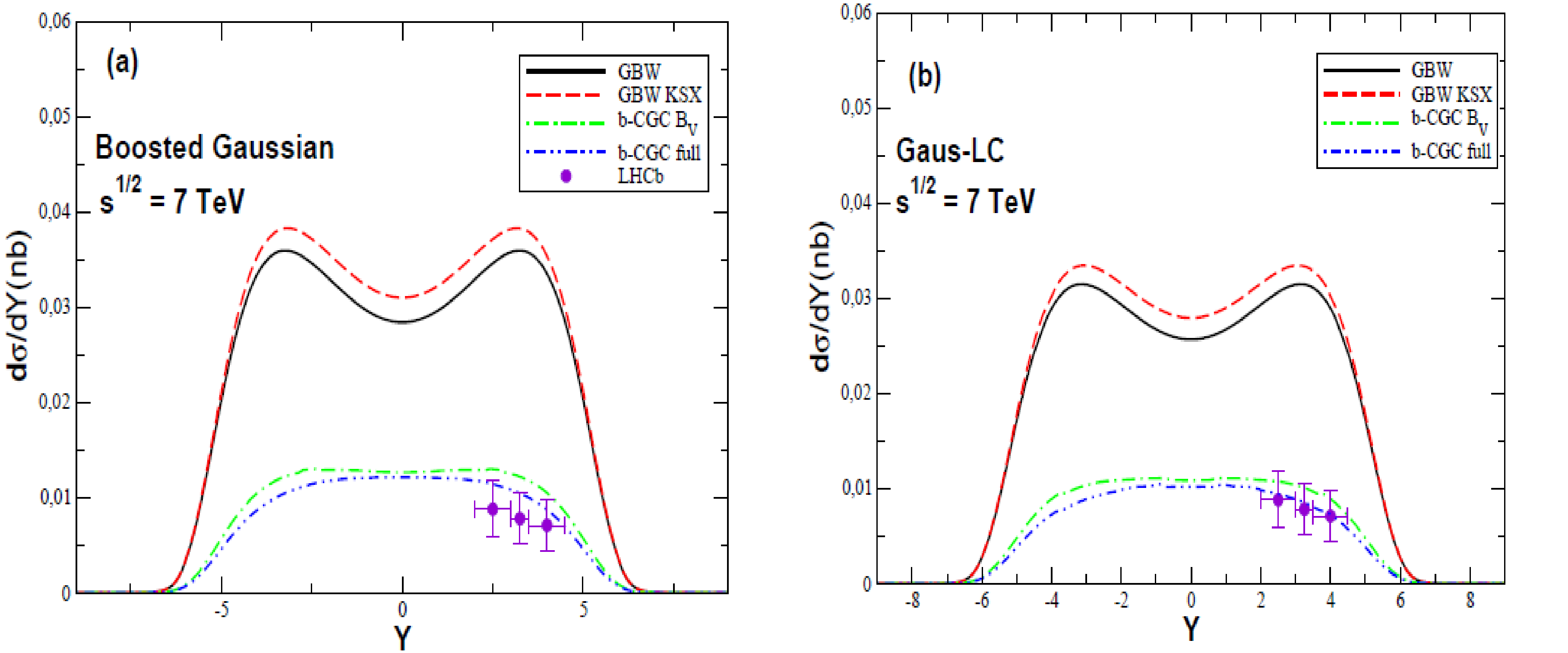

[b] VPG, Moreira, Navarra, PLB 472, 172 (2015)